



## BAWLD-CH<sub>4</sub>: A Comprehensive Dataset of Methane Fluxes from Boreal and Arctic Ecosystems

McKenzie A. Kuhn<sup>1</sup>, Ruth K. Varner<sup>2,3</sup>, David Bastviken<sup>4</sup>, Patrick Crill<sup>5,6</sup>, Sally MacIntyre<sup>7</sup>, Merritt  
5 Turetsky<sup>8</sup>, Katey Walter Anthony<sup>9</sup>, Anthony D. McGuire<sup>10</sup>, and David Olefeldt<sup>1</sup>.

<sup>1</sup> Department of Renewable Resources, University of Alberta. T6E 1V6, Edmonton, Alberta, Canada

<sup>2</sup> Department of Earth Sciences and Earth System Research Center, Institute for the Study of Earth, Oceans and Space,  
University of New Hampshire, Durham, NH 03824 USA

<sup>3</sup> Department of Physical Geography, Stockholm University, 10691 Stockholm, Sweden

10 <sup>4</sup> Department of Thematic Studies – Environmental Change, Linköping University, SE-581 83 Linköping, Sweden

<sup>5</sup> Department of Geological Sciences, Stockholm University, Stockholm, Sweden

<sup>6</sup> Bolin Centre for Climate Research, Stockholm, Sweden

<sup>7</sup> Marine Science Institute, University of California at Santa Barbara, Santa Barbara, USA

<sup>8</sup> Institute of Arctic and Alpine Research (INSTAAR), University of Colorado Boulder, Boulder, CO, USA.

15 <sup>9</sup> Water and Environmental Research Center, University of Alaska Fairbanks, PO Box 755860, Fairbanks, Alaska 99775-5860,  
USA.

<sup>10</sup> Institute of Arctic Biology, University of Alaska Fairbanks, Fairbanks, Alaska 99775, USA

*Correspondence to:* McKenzie Kuhn (kuhn.mckenzie@gmail.com)



20 **Abstract.** Methane (CH<sub>4</sub>) emissions from the Boreal and Arctic region are globally significant and highly sensitive to climate  
change. There is currently a wide range in estimates of high-latitude annual CH<sub>4</sub> fluxes, where estimates based on land cover  
inventories and empirical CH<sub>4</sub> flux data or process models (bottom-up approaches) generally are greater than atmospheric  
inversions (top-down approaches). A limitation of bottom-up approaches has been the lack of harmonization between  
inventories of site-level CH<sub>4</sub> flux data and the land cover classes present in high-latitude spatial datasets. Here we present a  
25 comprehensive dataset of small-scale, surface CH<sub>4</sub> flux data from 540 terrestrial sites (wetland and non-wetland) and 1247  
aquatic sites (lakes and ponds), compiled from 189 studies. The Boreal-Arctic Wetland and Lake Methane Dataset (BAWLD-  
CH<sub>4</sub>) was constructed in parallel with a compatible land cover dataset, sharing the same land cover classes to enable refined  
bottom-up assessments. BAWLD-CH<sub>4</sub> includes information on site-level CH<sub>4</sub> fluxes, but also on study design (measurement  
method, timing, and frequency) and site characteristics (vegetation, climate, hydrology, soil, and sediment types, permafrost  
30 conditions, lake size and depth, and our determination of land cover class). The different land cover classes had distinct CH<sub>4</sub>  
fluxes, resulting from definitions that were either based on or co-varied with key environmental controls. Fluxes of CH<sub>4</sub> from  
terrestrial ecosystems were primarily influenced by water table position, soil temperature, and vegetation composition, while  
CH<sub>4</sub> fluxes from aquatic ecosystems were primarily influenced by water temperature, lake size, and lake genesis. Models could  
explain more of the between-site variability in CH<sub>4</sub> fluxes for terrestrial than aquatic ecosystems, likely due to both less precise  
35 assessments of lake CH<sub>4</sub> fluxes and fewer consistently reported lake site characteristics. Analysis of BAWLD-CH<sub>4</sub> identified  
both land cover classes and regions within the Boreal and Arctic domain where future studies should be focused, alongside  
methodological approaches. Overall, BAWLD-CH<sub>4</sub> provides a comprehensive dataset of CH<sub>4</sub> emissions from high-latitude  
ecosystems that are useful for identifying research opportunities, for comparison against new field data, and model  
parameterization or validation. BAWLD-CH<sub>4</sub> can be downloaded from <https://doi.org/10.18739/A27H1DN5S>.

40



## 1 Introduction

Methane (CH<sub>4</sub>) is a strong climate forcing trace gas that is naturally produced and emitted from wetlands and lakes, which are abundant in northern regions (Matthews and Fung 1987; Lehner and Doll et al. 2004; Messenger et al. 2016). Current estimates of CH<sub>4</sub> fluxes from the northern Boreal and Arctic region (~>50°) range between 9 and 53 Tg CH<sub>4</sub> y<sup>-1</sup> from wetlands (Spahni et al. 2011; McGuire et al. 2012; Zhu et al. 2013; Bruhwiler et al. 2014; Treat et al. 2018; Watts et al. 2014; Thompson et al. 2017; Peltola et al. 2019; Saunois et al. 2020) and between 12 and 24 Tg CH<sub>4</sub> y<sup>-1</sup> from lakes (Bastviken et al. 2011; Wik et al. 2016a; Tan et al. 2016; Walter Anthony et al. 2016; Matthews et al. 2020; Saunois et al. 2020). Combined, CH<sub>4</sub> emissions from northern ecosystems make up a significant but uncertain portion of global wetland and freshwater fluxes (211-402 Tg CH<sub>4</sub> Yr<sup>-1</sup>) (Saunois et al. 2020). One reason for the large range of high latitude CH<sub>4</sub> emissions estimates is the consistently lower estimates based on top-down approaches compared to bottom-up approaches. Top-down approaches use atmospheric observations of CH<sub>4</sub> concentrations with atmospheric-inverse modeling frameworks to estimate regional CH<sub>4</sub> budgets (e.g. Bruhwiler et al. 2014; Thompson et al. 2017) while bottom-up approaches merge land cover datasets and empirical CH<sub>4</sub> flux inventories or process-based models to scale emissions across regional scales (e.g. Wik et al. 2016a; Treat et al. 2018; Peltola et al. 2019). A key issue for bottom-up approaches is the lack of differentiation among different wetland and lake types despite clear evidence indicating differences in both the magnitude and drivers of CH<sub>4</sub> fluxes among wetland and lake types (Olefeldt et al. 2013; Turetsky et al. 2014; Wik et al. 2016a; Treat et al. 2018).

Net CH<sub>4</sub> flux to the atmosphere depends on a suite of physical and biological controls linked to microbial production, oxidation, and transport via diffusion, ebullition, and plant-mediated processes (Bastviken et al. 2004; Whalen et al. 2005). While the basic underlying CH<sub>4</sub> processes are the same across all ecosystems, the dominance of different production, oxidation, and transport pathways vary within and among terrestrial (wetlands and non-wetlands) and lentic open-water aquatic ecosystems (lakes and ponds), leading to a wide range of reported CH<sub>4</sub> fluxes at the site level with differences of up to four orders of magnitude, including CH<sub>4</sub> uptake (Olefeldt et al. 2013; Wik et al. 2016a; Treat et al. 2018). Despite the wide range in reported CH<sub>4</sub> fluxes, key over-arching controls on emissions from wetlands and aquatic ecosystems have been identified through the work of syntheses (Olefeldt et al. 2013; Wik et al. 2016a; Treat et al. 2018), suggesting that different ecosystems can be partitioned based on a handful of key CH<sub>4</sub>-emitting characteristics.

For terrestrial ecosystems, CH<sub>4</sub> fluxes across the Boreal-Arctic region are primarily linked to permafrost conditions and hydrology (Olefeldt et al. 2013; Treat et al. 2018) which encompass other important controls on CH<sub>4</sub> emissions. For example, permafrost condition and hydrology can be directly linked to water table position and redox conditions (Moore et al. 1994; von Fischer et al. 2010; Olefeldt et al. 2017), which in turn influence plant composition (i.e. plant function types including graminoids, *Sphagnum* mosses, shrubs, and trees; Olefeldt et al. 2013; Bridgham et al. 2013), microbial community composition (McCalley et al. 2014), productivity (Öquist and Nykänen et al. 2003), and organic matter availability (Wagner et al. 2003; Christensen et al. 2003). Both permafrost condition and hydrology can further be used as an indication of soil temperature with typically colder soils in drier soils and permafrost-dominated landscapes (Olefeldt et al. 2017). Methane



fluxes are typically highest from graminoid-dominant wetlands like marshes and fens which are frequently inundated, which  
75 in turn enhances primary productivity (Ström et al. 2012), creates a soil habitat conducive to CH<sub>4</sub>-producing microbes  
(Woodcroft et al. 2018), and facilitates transport CH<sub>4</sub> through aerenchymatous roots and stems (Chanton et al. 1993; Ström  
and Christensen, 2007). Conversely, CH<sub>4</sub> fluxes are typically low from permafrost bogs and bogs which tend to have colder  
(in the case of permafrost bogs) and drier soil conditions (Beylea and Baird, 2006; Anderson et al. 2011), which are less  
conducive to the presence of graminoid species and promote the consumption of CH<sub>4</sub> through oxidation (Bartlett et al. 1992;  
80 Moosavi and Crill, 1997).

Methane fluxes from aquatic ecosystems (lakes and ponds) are highly influenced by lake morphology (Rasilo et al.  
2015; Holgerson and Raymond, 2016) and lake genesis (Wik et al. 2016a), including underlying permafrost conditions (Walter  
et al. 2006), which are associated with other key controls and CH<sub>4</sub> fluxes. Lake morphology influences sediment temperature,  
85 macrophyte presence (Marinho et al. 2015; Wik et al. 2018), and turbulent transfer (MacIntyre et al. 2018). Lake morphology,  
permafrost condition, and lake genesis all determine organic substrate availability in sediments (Walter et al. 2006, Wik et al.  
2016a) and trophic status (Bastviken et al. 2004; DelSontro et al. 2016). For example, peatland lakes and ponds, which form  
through degradation and permafrost thaw processes in peatlands, are relatively high CH<sub>4</sub> emitters (Matveev et al. 2016; Kuhn  
et al. 2018; Burke et al., 2019). These waterbodies are underlain by organic-rich sediments and are typically small and shallow  
90 and less likely to be seasonally stratified, allowing for rapid sediment warming and carbon mineralization (Matveev et al.  
2016). Glacial and post-glacial waterbodies, on the other hand, have relatively low CH<sub>4</sub> fluxes due to deeper water columns,  
which limit ebullition, and also have mineral-rich sediments with typically less labile organic substrates (Schnurrenberger et  
al. 2003; DelSontro et al. 2016; Wik et al. 2016a). Therefore, while there are many physical and biogeochemical controls on  
aquatic CH<sub>4</sub> fluxes, size and lake genesis can be useful proxies for many of these underlying factors.

95 There are various methodologies used to measure surface CH<sub>4</sub> fluxes from terrestrial and aquatic ecosystems. Two  
approaches used in both terrestrial and aquatic ecosystems include micrometeorological eddy covariance (EC) techniques  
and chamber measurement techniques. Eddy covariance measurements are collected at high temporal frequencies from  
towers and typically cover a footprint of 100-10,000 m<sup>2</sup>. The near-continuous nature of EC measurements provide valuable  
insight into the temporal patterns and drivers of CH<sub>4</sub> fluxes, however, towers are geographically limited across the Boreal-  
100 Arctic region and it can be difficult to attribute flux transport pathways and specific source areas at fine spatial scales  
(Delwiche et al. 2021; Knox et al. 2019). Conversely, static chamber measurements cover small spatial areas that allow for  
detailed assessments of environmental controls on fluxes (Olefeldt et al. 2013; Bäckstrand et al. 2008). Chamber-based  
methods quantify fluxes by calculating the change in chamber headspace concentration over a set time, which varies based  
on extraction methods (i.e. syringe, automated chamber, or portable gas analyzer). While chamber-based techniques have  
105 drawbacks, including surface disturbance, typically low sampling frequency, and high labor intensity, they are easily  
installed, can capture environmental controls of CH<sub>4</sub> fluxes at a sub-meter scale, and are cheaper options compared to  
installing and maintaining EC towers. Thus, we focus mostly on chamber-based flux measurements in this synthesis because



they have been performed at a large number of sites across the Boreal and Arctic region and represent more of the geographic variation across the region.

110 In aquatic ecosystems, turbulence-driven modeling approaches, inverted funnels (i.e. bubbles traps), and ice bubble surveys (IBS) are additionally used to quantify fluxes. Modeling approaches calculate net hydrodynamic flux (herein referred to as diffusion) to the atmosphere by determining the concentration of dissolved CH<sub>4</sub> in the water column and an estimate of the gas transfer velocity  $k$  (See Sect. 2.4 for more information). Bubble traps capture the volume of bubble gas released from sediments; ebullitive flux can be estimated by using the concentration of CH<sub>4</sub> found in the bubble (Wik et al. 2013). Finally, 115 IBS are used to quantify the spatial abundance and types of bubble formations trapped within lake ice over the winter (Walter et al. 2010). Importantly, these surface-based methods can be used to assess controls of CH<sub>4</sub> exchange at scales of individual ponds, lakes, and portions of open-water wetlands, providing key insights into the environmental processes controlling CH<sub>4</sub> flux to the atmosphere (Olefeldt et al. 2013; Wik et al. 2016a).

Here we expanded, updated, and merged previous CH<sub>4</sub> flux syntheses for northern wetlands (Olefeldt et al. 2013) 120 and lakes (Wik et al. 2016a) to create a small-scale (sub-meter), surface-based dataset for CH<sub>4</sub> fluxes collected from 189 studies across the Boreal-Arctic region. The dataset was built in parallel with a novel, CH<sub>4</sub>-specific land cover dataset for the circumpolar north- the Boreal-Arctic Wetland and Lake Dataset (BAWLD; Olefeldt et al. 2021), allowing for flux observations and spatial distribution of land cover features to be classified under the same criteria for the first time at a pan-Arctic scale. This dataset provides an open platform for surface-based fluxes and associated environmental drivers from aquatic, wetland, 125 and upland (i.e. non-wetland) ecosystems and can be utilized by both field researchers and the modeling community. Information in the dataset can be used to compare field results, identify new research opportunities, or build and test models. This dataset includes and uniformly classifies lake, wetland, and upland (non-wetland) surface CH<sub>4</sub> flux data for the circumpolar north. In this study, we show CH<sub>4</sub> flux distributions and environmental drivers from various terrestrial (wetland and upland) and aquatic ecosystems, compare the results to previous CH<sub>4</sub> flux syntheses, highlight key gaps in the data, and 130 suggest future research directions.

## 2 Dataset description and BAWLD land cover classification

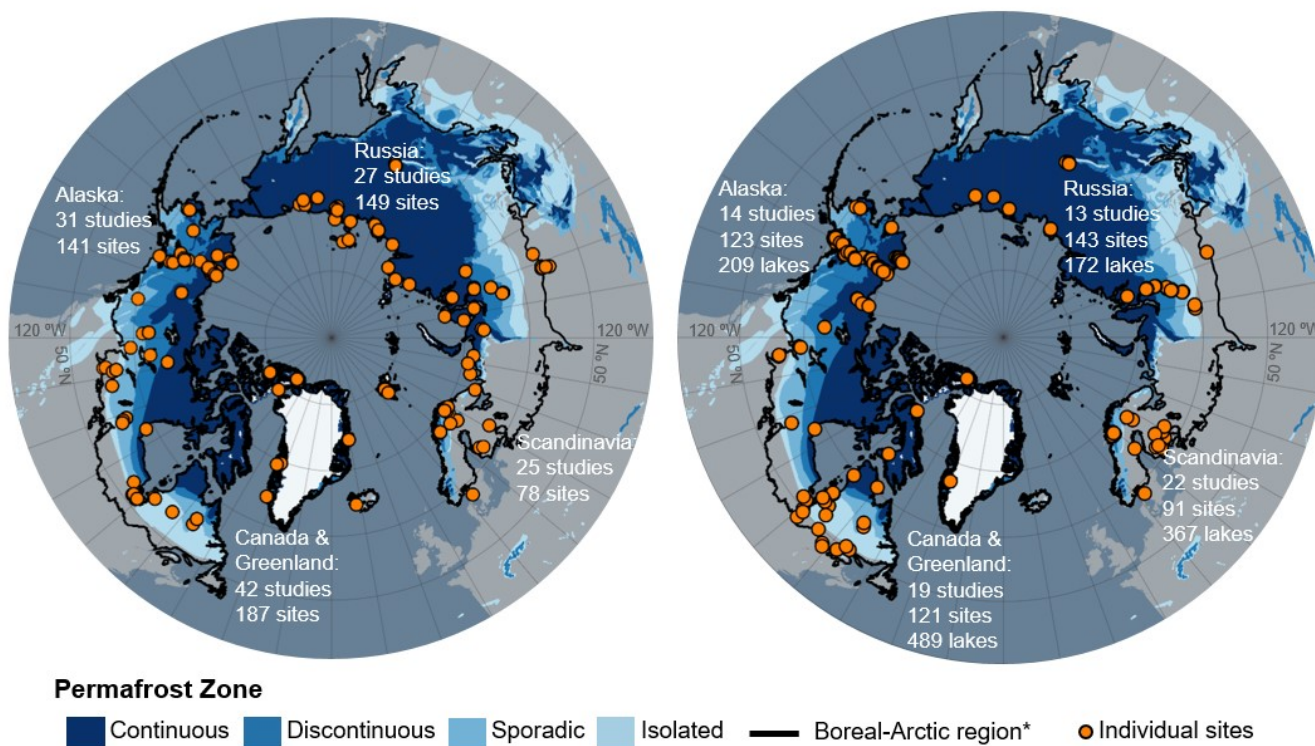
The dataset is composed of two parts including 1) terrestrial ecosystems (vegetated wetland and non-wetland ecosystems) and 2) lentic open-water aquatic ecosystems (lakes, ponds, and open water pools; hereafter referred to as “aquatic ecosystems”). This synthesis does not include lotic systems (streams and rivers), which are already synthesized in Stanley et al. (2015). The datasets for terrestrial and aquatic ecosystems are reported as separate components due to differences between 135 both the drivers of CH<sub>4</sub> fluxes and data collection methods. The terrestrial dataset extends the work by Olefeldt et al. (2013), who compiled CH<sub>4</sub> flux estimates for wetlands in the permafrost zones designated by Brown et al (2002). Our dataset expands on this initial work to include flux data from non-permafrost and non-wetland sites throughout the Arctic and Boreal region (Olson et al. 2001) and flux data from studies between 2012 and February 2020. We updated the initial dataset to include 140 separate entries for individual sites that reported flux and water table data for multiple years. We expanded the number of site-



year flux estimates in the original terrestrial dataset by 83% and expanded the number of independent studies by 86%, leading to a total of 555 warm-season (~May through October depending on the location) flux estimates and 121 studies (Fig. 1a). The aquatic dataset extends the work by Wik et al. (2016a) which is a compilation of CH<sub>4</sub> flux data for lakes and ponds north of 50° N. We expand on this initial work to include studies between 2016 and February 2020. Additionally, we updated the original aquatic dataset to include the within-lake location for ebullition measurements and the equation used to model the gas velocity coefficient *k*. We expanded the number of lakes in the dataset by 71% and the number of studies by 66%, summing to a total of 1251 lakes and 68 independent studies (Fig. 1b). Finally, each terrestrial and aquatic site was reclassified into a new land cover classification, further explained below.

(a) Terrestrial (121 studies)

(b) Aquatic (68 studies)



150 **Figure 1. Maps of the individual sites (orange circles) incorporated in BAWLD-CH<sub>4</sub>.** a) Sites included in the terrestrial flux dataset. b) Sites included in the aquatic flux dataset. The number of “sites” in the terrestrial data set represents site-years, which in some cases represent multiple years of data from one site or data from the same site reported by different studies. “Sites” in the aquatic dataset represent the reported average fluxes for one or multiple lakes. In some cases, studies reported one mean value for multiple lakes, therefore the number of lakes and the number of sites are not the same. \*Boreal-Arctic Region boundary from Olson et al. 2001. Permafrost zones are from Brown et al. 2002. Continental shoreline base layers are from Wessel et al. 1996.

### 2.1.0 Land cover classes in the Boreal Arctic Wetland and Lake Dataset

Land cover classes in the Boreal-Arctic Wetland and Lake Dataset (BAWLD; Olefeldt et al. 2021) were chosen and defined to enable upscaling of CH<sub>4</sub> fluxes at large spatial scales. As such, we aimed to include as few classes as possible to facilitate



160 large-scale mapping, while still having sufficient classes to allow separation among groups of ecosystems with similarities in hydrology, ecology, and biogeochemistry and therefore net CH<sub>4</sub> fluxes. The BAWLD land cover classification is hierarchical; with four upland classes, five wetland classes, seven lentic aquatic classes, and three lotic aquatic classes. As mentioned previously, fluxes from lotic ecosystems (streams and rivers) are not been included in this dataset but are covered by Stanley et al. (2015).

### 2.1.1 Wetland Classes

165 Wetlands are defined by having a water table near or above the land surface for sufficient time to cause the development of wetland soils (either mineral soils with redoximorphic features, or organic soils with > 40 cm peat), and the presence of plant species with adaptations to wet environments (Canada Committee on Ecological (Biophysical) Land Classification et al., 1997; Jorgenson et al., 2001; Hugelius et al., 2020). Wetland classifications for boreal and arctic biomes can focus either on small-scale wetland classes that have distinct hydrological regimes, vegetation composition, and biogeochemistry or on larger-scale wetland complexes that are comprised of distinct patterns of smaller wetland and open-  
170 water classes (Glaser et al., 2004; Masing et al., 2010; Gunnarsson et al., 2014; Terentieva et al., 2016). While larger-scale wetland complexes are easier to identify through remote sensing techniques (e.g. patterned fens comprised of higher elevation ridges and inundated hollows), our classification focuses on wetland classes due to greater homogeneity of hydrological, ecological, and biogeochemical characteristics that regulate CH<sub>4</sub> fluxes (Heiskanen et al., 2021).

175 Several boreal countries identify four main wetland classes, differentiated primarily based on hydrodynamic characterization; bogs, fens, marshes, and swamps (Canada Committee on Ecological (Biophysical) Land Classification et al., 1997; Masing et al., 2010; Gunnarsson et al., 2014). The BAWLD classification follows this general framework, but further uses the presence or absence of permafrost as a primary characteristic for classification and excludes a distinct swamp class, yielding five classes; *Bogs*, *Fens*, *Marshes*, *Permafrost Bogs*, and *Tundra Wetlands* (see Fig. 2 and Fig. 3). The swamp class  
180 was omitted due to the wide range of moisture and nutrient conditions of swamps, as well as the limited number of studies of swamp CH<sub>4</sub> fluxes. We instead included swamp ecosystems in expanded descriptions of *Bogs*, *Fens*, and *Marshes*. The presence or absence of near-surface permafrost was used as a primary characteristic to distinguish between *Permafrost Bogs* and *Bogs* and to distinguish *Tundra Wetlands* from *Marshes* and *Fens*. The presence or absence of near-surface permafrost is considered key for controlling CH<sub>4</sub> emissions given its influence on hydrology, and for the potential of permafrost thaw and  
185 thermokarst collapse to cause rapid non-linear shifts to CH<sub>4</sub> emissions (Bubier et al., 1995; Turetsky et al., 2002; Malhotra and Roulet, 2015; Fig. 3). Finally, while some classifications include shallow (e.g. 2 m depth), open-water ecosystems within the definition of wetlands (Canada Committee on Ecological (Biophysical) Land Classification et al., 1997; Gunnarsson et al., 2014), we have included all open-water ecosystems without emergent vegetation within the lake classes (see below) due to the strong influence of emergent vegetation in controlling CH<sub>4</sub> emissions (Juutinen et al., 2003).

190

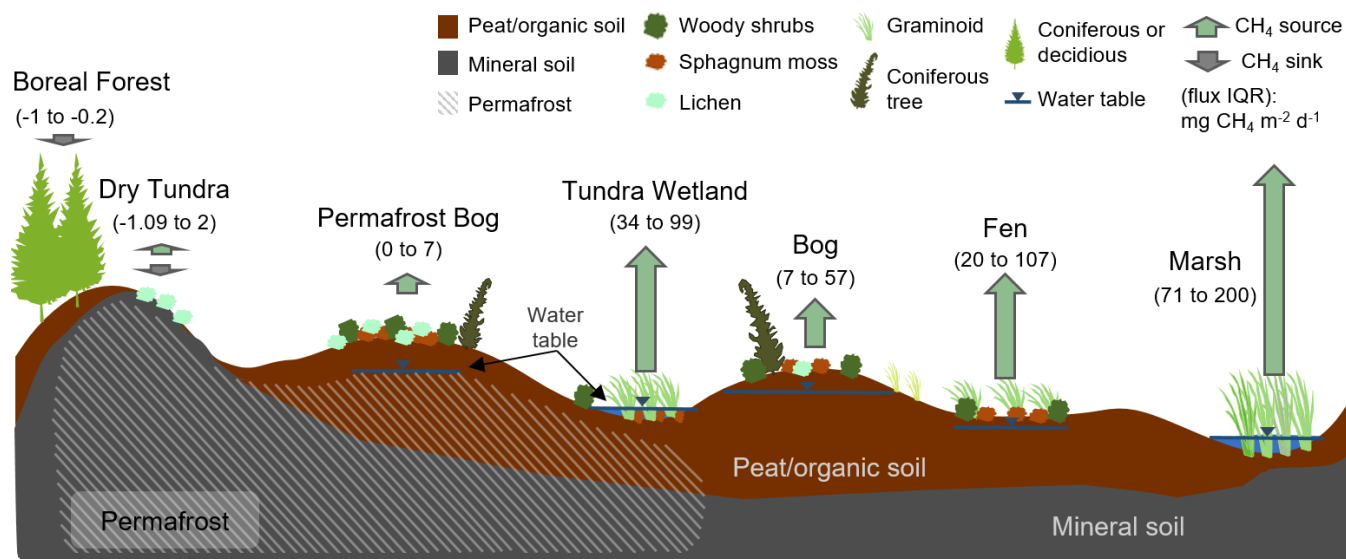


**Figure 2.** Conceptual diagram of the terrestrial land cover classes and their CH<sub>4</sub>-emitting characteristics including permafrost conditions, hydrology, organic layer depth, and associated nutrient and vegetation characteristics. Numbers within the brackets represent the interquartile (IQR) flux ranges. Arrows are scaled based on mean flux values. See Sect. 3.2 for a detailed breakdown of terrestrial fluxes.

195

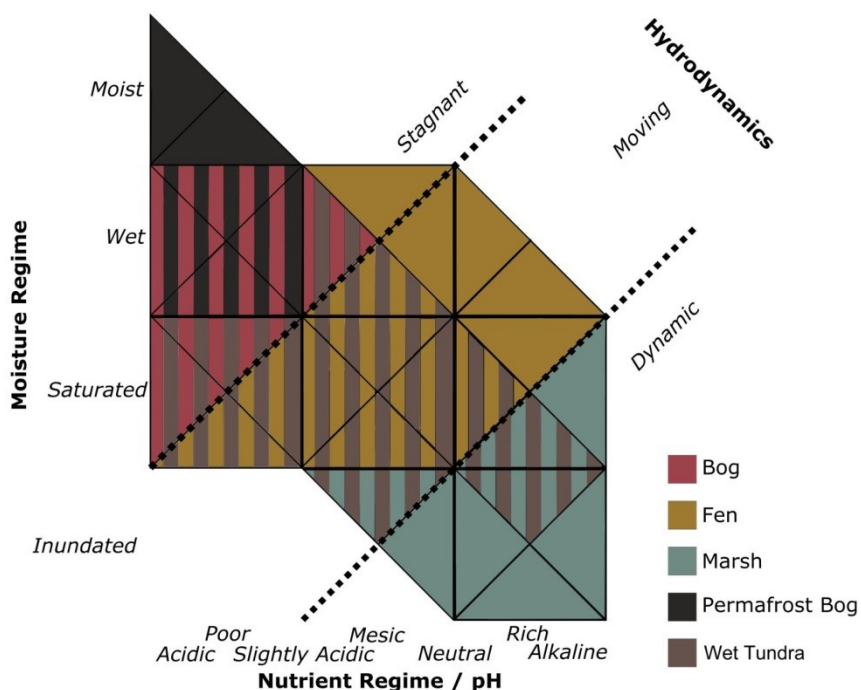


**Figure 3.** Definitions of the five wetland classes in BAWLD along axes of moisture regime and nutrient regime.



200 *Bogs* are described as ombrotrophic peatland ecosystems, i.e. only dependent on precipitation, and snowmelt for water  
inputs. Peat thickness is at least 40 cm, with maximum thickness > 10 m. The peat profile is not affected by permafrost,  
although in some climatically colder settings there may be permafrost below the peat profile. *Bogs* are wet to saturated  
ecosystems, often with small-scale (<10 m) microtopographic variability, with stagnant water and a water table that rarely is  
above the surface or more than 50 cm below the surface (Fig. 3). *Bogs* have low pH (<5), low concentrations of dissolved ions,  
205 and low nutrient availability resulting from a lack of hydrological connectivity to surrounding mineral soils. Vegetation is  
commonly dominated by *Sphagnum* mosses, lichens, and woody shrubs, and can be either treed or treeless (Beaulne et al.,  
2021). Our description of *Bogs* also includes what is commonly classified as treed swamps, which generally represent ecotonal  
transitions between peatlands and upland forests (Canada Committee on Ecological (Biophysical) Land Classification et al.,  
1997).

210 *Fens* are described as minerotrophic peatland ecosystems, i.e. hydrologically connected to surrounding mineral soils  
through surface water or groundwater inputs. A *Fen* peat profile is at least 40 cm thick (Gorham et al. 1991), although  
maximum peat thickness is generally less than for bogs. The peat profile is not affected by permafrost. *Fens* are wet to saturated  
ecosystems, with generally slow-moving water (Fig. 3). *Fens* have widely ranging nutrient regimes and levels of dissolved  
ions depending on the degree and type of hydrological connectivity to their surroundings, ranging from poor fens to rich fens.  
215 Vegetation largely depends on wetness and nutrient availability, where more nutrient-poor fens can have *Sphagnum* mosses,  
shrubs, and trees, while rich fens are dominated by brown mosses, graminoids (sedges, rushes), herbaceous plants, and  
sometimes coniferous or deciduous trees (e.g. willows, birch, larch). Our description of *Fens* also includes what is commonly  
classified as shrubby swamps, which often are associated with riparian ecotones and lake shorelines.

*Marshes* are minerotrophic wetlands with dynamic hydrology, and often high nutrient availability (Fig. 3). Vegetation  
220 is dominated by emergent macrophytes, including tall graminoids such as rushes, reeds, grasses, and sedges – some of which  
can persist in settings with >1.5 m of standing water. *Marshes* are saturated to inundated wetlands, often with highly fluctuating  
water levels as they generally are located along shorelines of lakes or coasts, along streams and rivers, or on floodplains and  
deltas. It is common for marshes to exhibit both flooded and dry periods. Dry periods facilitate the decomposition of organic  
matter and can prevent the build-up of peat. As such *Marshes* generally have mineral soils, although some settings allow for  
225 the accumulation of highly humified organic layers – sometimes indicating ongoing succession towards a peatland ecosystem.  
Salinity can vary depending on water sources, with brackish to saline conditions in some areas of groundwater discharge, or  
in coastal settings.

*Permafrost Bogs* are peatland ecosystems, although the peat thickness in cold climates is often relatively shallow.  
*Permafrost Bogs* have a seasonally thawed active layer that is 30 to 70 cm thick, with the remainder of the peat profile  
230 perennially frozen (i.e. permafrost). Excess ground-ice and ice expansion often elevate *Permafrost Bogs* up to a few meters  
above their surroundings, and as such, they are ombrotrophic and generally the wetland class with the driest soils (Fig. 3).  
*Permafrost Bogs* have moist to wet soil conditions, often with a water table that follows the base of the seasonally developing  
thawed soil layer. Ombrotrophic conditions cause nutrient-poor conditions, and the vegetation is dominated by lichens,



235 *Sphagnum* mosses, woody shrubs, and sometimes stunted coniferous trees. *Permafrost Bogs* are often interspersed in a fine-scale mosaic (10 to 100 m) with other wetland classes, e.g. *Bogs* and *Fens*. Common *Permafrost Bog* landforms include palsas, peat plateaus, and the elevated portions of high- and low-center polygonal peatlands.

240 *Tundra Wetlands* are treeless ecosystems with saturated to inundated conditions, most commonly with near-surface permafrost (Fig. 3). *Tundra Wetlands* can have either mineral soils or shallow organic soils, and generally receive surface or near-surface waters from their surroundings, as permafrost conditions preclude connectivity to deeper groundwater sources. Vegetation is dominated by short emergent vegetation, including sedges and grasses, with mosses and shrubs in slightly drier sites. *Tundra Wetlands* have a lower maximum depth of standing water than *Marshes*, due to the shorter vegetation. *Tundra Wetlands* can be found in basin depressions, in low-center polygonal wetlands, and along rivers, deltas, lake shorelines, and on floodplains in regions of continuous permafrost. Despite the name, limited wetlands with these characteristics (hydrology, permafrost conditions, and vegetation) can also be found within the continuous permafrost zone in boreal and sub-arctic regions  
245 (Virtanen et al., 2016).

### 2.1.2 Upland and Other Classes

Upland and other classes in BAWLD; *Glaciers*, *Rocklands*, *Dry Tundra*, and *Boreal Forests*, have in common that they are neither wetlands nor aquatic ecosystems. *Glaciers* are assumed to have neutral CH<sub>4</sub> fluxes, however, to our knowledge there are no published studies with field data. *Rocklands* are also expected to have very low CH<sub>4</sub> fluxes (Oh et al. 2020),  
250 potentially with more frequent CH<sub>4</sub> uptake than release – however, there were very few sites that fit within this class (n=5), therefore these flux estimates were combined with *Dry Tundra* sites.

The *Dry Tundra* class includes both lowland arctic tundra and alpine tundra; both treeless ecosystems dominated by graminoid or shrub vegetation. *Dry Tundra* ecosystems generally have near-surface permafrost, with seasonally thawed active layers between 20 and 150 cm depending on climate, soil texture, and landscape position (van der Molen et al., 2007; Heikkinen et al., 2004). Near-surface permafrost in *Dry Tundra* prevents vertical drainage, but lateral drainage ensures predominately oxic soil conditions. A water table is either absent or close to the base of the seasonally thawing active layer. *Dry Tundra* is differentiated from *Permafrost Bogs* by having thinner organic soil (<40 cm), and from *Tundra Wetlands* by their drained soils (average water table position >5 cm below soil surface).

260 *Boreal Forests* are treed ecosystems with non-wetland soils. Coniferous trees are dominant, but the class also includes deciduous trees in warmer climates and landscape positions. *Boreal Forests* may have permafrost or non-permafrost ground, where the absence of permafrost often allows for better drainage. Overall, it is rare for anoxic conditions to occur in *Boreal Forest* soils, and CH<sub>4</sub> uptake is prevalent, although low CH<sub>4</sub> emissions have been observed during brief periods during snowmelt or following summer storms (Matson et al., 2009), or conveyed through tree stems and shoots (Machacova et al., 2016). The *Boreal Forest* class also includes the few agricultural/pasture ecosystems within the boreal biome.



### 265 2.1.3 Aquatic Classes

Lakes in BAWLD include all lentic open-water ecosystems (herein referred to as aquatic ecosystems), regardless of surface area and depth of standing water. It is common in ice-rich permafrost lowlands and peatlands for open-water bodies to have shallow depths, often less than two meters, even when surface areas are up to hundreds of km<sup>2</sup> in size (Grosse et al., 2013). While small, shallow open-water bodies often are included in definitions of wetlands (Gunnarsson et al., 2014; Treat et al., 2018; Canada Committee on Ecological (Biophysical) Land Classification et al., 1997), we include them here within the lake classes as controls on net CH<sub>4</sub> emissions depend strongly on the presence or absence of emergent macrophytes (Juutinen et al., 2003). Further classification of lakes in BAWLD is based on lake size and lake genesis, where lake genesis influences lake bathymetry and sediment characteristics (Fig. 4). Previous global spatial inventories of lakes include detailed information on size and location of individual larger lakes (Downing et al., 2012; Messenger et al., 2016), but do not include open-water ecosystems <0.1 km<sup>2</sup> in size, and do not differentiate between lakes of different genesis (e.g. tectonic, glacial, organic, and yedoma lakes). Small water bodies are disproportionately abundant in some high latitude environments (Muster et al., 2019), have high emissions of CH<sub>4</sub> (Holgerson and Raymond, 2016), and therefore require explicit classification apart from larger water bodies. Furthermore, lake genesis and sediment type have been shown to influence net CH<sub>4</sub> flux from lakes (Wik et al., 2016a). In BAWLD we thus differentiate between large (>10 km<sup>2</sup>), midsize (0.1 to 10 km<sup>2</sup>), and small (<0.1 km<sup>2</sup>) lake classes, and further differentiate between three lake types for midsize and small lakes; peatland, yedoma, and glacial lakes (Fig. 4).

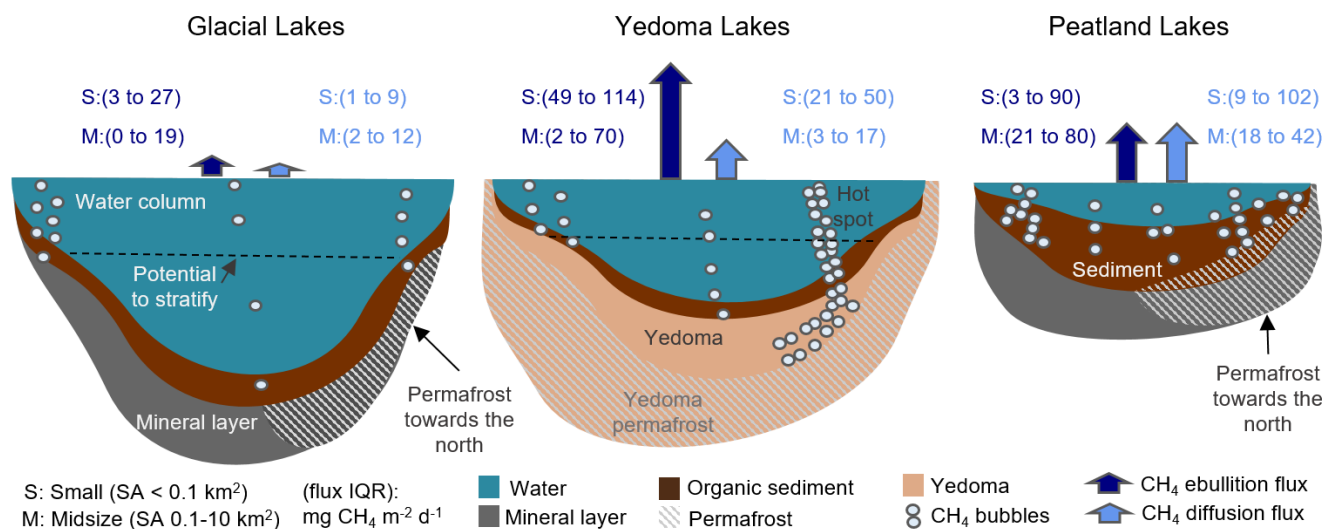


**Figure 4. Conceptual diagram of the aquatic land cover classes.** Key differences between the three overarching lake genesis “types” and their CH<sub>4</sub>-emitting characteristics are shown, including sediment type, permafrost conditions, and water column depth. Fluxes (interquartile ranges-IQR) for each class size within the overarching types are shown above the lakes for both diffusive and ebullitive transport pathways. Arrows are scaled based on mean flux values. See Sect. 3.3 for a detailed breakdown of aquatic fluxes. *Large lakes* are not shown.

*Small and Midsize Peatland Lakes* are described as lakes with thick organic sediments that are mainly found adjacent to or surrounded by peatlands, or in lowland tundra regions with organic-rich soils. *Small Peatland Lakes* includes the



290 numerous small pools often found in extensive peatlands and lowland tundra regions, e.g. including the open-water parts of string fens and polygonal peatlands. *Peatland Lakes* generally form as a result of interactions between local hydrology and the accumulation of peat which can create open water pools and lakes (Garneau et al., 2018; Harris et al., 2020), but can also form in peatlands as a result of permafrost dynamics (Sannel and Kuhry, 2011; Liljedahl et al., 2016). As such, these lakes with thick organic sediments are often shallow and have a relatively low shoreline development index. *Peatland lakes* typically have dark waters with high concentrations of dissolved organic carbon.

295 *Small and Midsize Yedoma Lakes* are exclusive to non-glaciated regions of eastern Siberia, Alaska, and the Yukon where yedoma deposits accumulated during the Pleistocene (Strauss et al., 2017). Yedoma permafrost soils are ice-rich and contain fine-grained, organic-rich loess that was deposited by wind and accumulated upwards in parallel with permafrost aggradation, thus limiting decomposition and facilitating organic matter burial (Schirrmeister et al., 2013). Notable thermokarst features, including lakes, often develop when yedoma permafrost thaws, causing labile organic matter to become available for microbial mineralization (Walter Anthony et al., 2016). *Small Yedoma Lakes* are thus more likely to have actively thawing and  
300 expanding lake edges where CH<sub>4</sub> emissions can be extremely high, largely driven by hot spot ebullition emissions (Walter Anthony et al., 2016; Fig. 4). Century-scale development of yedoma lakes can shift the main source of CH<sub>4</sub> production from yedoma deposits to new organic-rich sediment that accumulated from allochthonous and autochthonous sources – resulting in such lakes here being considered as *Peatland Lakes*.

305 *Small and Midsize Glacial Lakes* include all lakes with organic-poor sediments – predominately those formed through glacial or post-glacial processes, e.g. kettle lakes and bedrock depressions. However, due to similarities in CH<sub>4</sub> emissions and controls thereof, we also include all other lakes with organic-poor sediments within these classes. *Glacial Lakes* typically have rocky bottoms or mineral sediments with limited organic content. Lakes in this class are abundant on the Canadian Shield and in Scandinavia but can be found throughout the boreal and tundra biomes. Many *Glacial Lakes* have a high shoreline development index, with irregular, elongated shapes. Generally, *Glacial Lakes* are deeper than lakes in the other classes, when  
310 comparing lakes with similar lake areas and are more likely to stratify seasonally than peatland lakes (Fig. 4).

*Large Lakes* are greater than 10 km<sup>2</sup> in surface area. Most *Large Lakes* are glacial or structural/tectonic in origin. Lake genesis is not considered for further differentiation within this land cover class.

## 2.2 Terrestrial Methane Flux Dataset

315 The terrestrial CH<sub>4</sub> flux dataset includes warm-season (~May-October depending on the location) fluxes and was compiled using data from studies published before February 2020. We identified relevant studies using 1) JStore™, Google Scholar™ and Web of Science™ searches with the terms (peatland OR wetland OR bog OR fen OR marsh OR upland) AND (north\* OR boreal OR arctic OR sub-arctic) AND (methane OR CH<sub>4</sub> OR greenhouse gas\*); 2) references from published studies; and 3) contributions of unpublished data (n=1). If multiple, yearly CH<sub>4</sub> flux and water table measurements were reported from one site or if multiple studies reported fluxes from the same site, the data were entered as separate individual  
320 lines and were considered each their own “site.” Sites that underwent manipulations (soil temperature, water table, nutrients,



etc.) were not included in the dataset, however, any control or undisturbed sites included within manipulation studies were included. Sites that had recently experienced disturbance from thermokarst processes were included. Winter flux measurements from terrestrial sites were excluded from this dataset (winter/ice-out emissions from aquatic ecosystems are included- see Sect. 2.3). A comprehensive synthesis of seasonal winter estimates of CH<sub>4</sub> emissions from northern terrestrial ecosystems are presented in Treat et al. (2018).

The terrestrial dataset includes predominantly chamber measurements (n=519) at the sub-meter scale which allows for a detailed representation of specific land cover classes (i.e. one land cover class per chamber measurement). However, a handful of eddy covariance measurements were included if the authors could clearly partition fluxes based on specific land cover classes (n=36). For more information on EC-based CH<sub>4</sub> synthesis, we direct the readers to the FLUXNET-CH<sub>4</sub> Community Product (Delwiche et al. 2021; Knox et al. 2019) and additional FluxNet resources (fluxnet.org). We grouped chamber measurements from specific studies by “Site”, which we defined as surfaces with similar vegetation composition (dominant, present, absent) and physical characteristics (including water table position, permafrost conditions, organic layer depth, soil moisture, and pH) within proximity to each other (typically 1 – 100 m radius). In most cases, chambers and sites were already classified by these standards, however, sometimes it was necessary to combine or split chamber measurements presented by the authors into our site and classifications. By combining and splitting sites this way, we were able to classify sites into BAWLD land cover classes. Average daily warm-season fluxes were then calculated from the average CH<sub>4</sub> flux from each site over the study’s measurement period.

In addition to CH<sub>4</sub> flux data, we extracted various site descriptors and categorical and continuous environmental variables (See Table 1 for detailed attribute information and additional variables not discussed here). For all sites, we included information on the site name (Site), location (LatDec/LongDec, Country), the months measurements were taken (SampMonths), the flux measurement method (Meth), the author’s description of the site (SiteDescrip), and vegetation composition. Most studies did not classify land cover types with similar BAWLD criteria, therefore we assigned BAWLD land cover classifications. Permafrost zone was assigned according to Brown et al. (2002). When reported by the authors, we also extracted continuous variables including Mean Annual Air Temperature (MAAT), Mean Annual Precipitation (MAP), growing season length, Net Ecosystem Productivity (NEP), Ecosystem Respiration (ER), Gross Ecosystem Photosynthesis (GPP<sub>Per</sub>), air temperature (T<sub>Per</sub>), soil temperature at 0-5 cm (T<sub>SoilA</sub>) and at 5-25 cm (T<sub>SoilB</sub>), water table depth (WT<sub>Av</sub>), organic layer depth (Org), active layer depth (AL), pH, and soil moisture (SoilMoist), all averaged over the same period as the flux measurements. The categorical variables collected include absence or presence of permafrost within the top two meters (PfConA), permafrost thaw (PfTh), and vegetation composition (absent, present, dominant) for graminoid (*Carex spp.* and *Eriophorum spp.*; referred to as “Sedge” in the dataset), sphagnum moss (Sphag), non-sphagnum moss (Moss), tree, and shrub species. Vegetation composition of the functional plant type was considered dominant if that type made up greater than 50% of the reported biomass or areal coverage or was one of only two species present at the site. Trees were assigned as the dominant vegetation type if the canopy was described as closed. Gridded (0.5 by 0.5 degrees) climate variables including mean



355 annual temperature (referred to as GRID\_T) and mean annual precipitation (CD\_Pcp\_An) were extracted from WorldClim2 (<http://www.worldclim.com/version2>).

**Table 1. Attribute information for the terrestrial flux dataset.**

Column_Name	Variable_Name	Units_Info	Description	Controlled_Vocab
RefID	Reference ID	-	Number ID attached to independent publications	-
Dataset	Dataset Name	Olefeldt, Kuhn	Data entered originally included by Olefeldt et al or new data entered by Kuhn et al. All were updated to include additional information not include originally by Olefeldt et al.	Olefeldt, Kuhn
Reference	Reference	-	Author name and year published	-
LatDec	Latitude	Decimal Degrees	Coordinates given by the authors	-
LongDec	Longitude	Decimal Degrees	Coordinates given by the authors	-
Site	Site Name	-	Names of site provided by the authors	-
SiteID	Shortened SiteID	-	An abbreviated version of the site name	-
Country	Country	-	Country where the research took place	USA: United States, Canada, Russia, Sweden, Norway, Greenland, Finland
ID	Measurement location ID	-	Name of the individual plot	-
Ecosystem	Ecosystem Classification	-	Short name for the ecosystem type described by the authors	-
SiteDescrip	Site Description	-	A description of the site given by the authors	-
Class	Land cover Class	-	BAWLD land cover classification	Bog, Fen, Marsh, WetTundra (Tundra Wetlands), DryTundra, Boreal: Boreal Forest, PermBog = Permafrost bog
Seas	Season/s	T, S, F	Seasons the measurements took place in	T: Thaw/spring, S: Summer, F-fall
Year.P	Publication Year	Year	Year the study was published	-
Year.M	Measurement year/s	Year	Year/s the fieldwork took place	-
SampleDays	Sampling Days	Days	Number of measurement days	-
Month.Numbers	Number of sampling months	Months	The number of months in which sampling occurred	-



SampMonths	Sampling Months	-	The months that sampling took place in	Jn: June, J: July, A: August, S: September, O: October
Meth	Method	C, E, CE	Methane flux measurement method	C: Chamber, E: Eddy Covariance
Coll	Collars	Number of collars	Number of collars used to estimate the average methane flux at a site	-
Occ	Occasions	Flux measurements	Number of times a flux was measured at an individual collar	-
GrowSL	Growing Season Length	Days	Length of the growing season as reported by the authors	-
CH4An	Annual Fluxes	$\text{g m}^{-2} \text{ yr}^{-1}$	Annual methane fluxes as reported by the authors	-
CH4Av	Average daily methane fluxes	$\text{mg CH}_4 \text{ m}^{-2} \text{ d}^{-1}$	Average growing season methane fluxes	-
CH4Md	Median daily methane flux	$\text{mg CH}_4 \text{ m}^{-2} \text{ d}^{-1}$	Median growing season flux, if reported by authors	-
CH4Mx	Max daily methane flux	$\text{mg CH}_4 \text{ m}^{-2} \text{ d}^{-1}$	Maximum methane flux over the growing season, if reported by authors	-
NEPPer	Net Ecosystem Primary Productivity	$\text{g C m}^{-2} \text{ yr}^{-1}$	-	-
ERPer	Ecosystem Respiration	$\text{g C m}^{-2} \text{ yr}^{-1}$	-	-
GPPPer	Gross Ecosystem Productivity	$\text{g C m}^{-2} \text{ yr}^{-1}$	-	-
MAAT	Mean Annual Temperature	Celsius	Meant Annual Temperature reported by the authors	-
MAP	Mean Annual Precipitation	mm	Meant Annual Precipitation reported by the authors	-
TPer	Air Temperature	Celsius	Reported air temperature at the time of the methane measurement	-
TSoilA	Surface Soil Temperature	Celsius	Temperature of the soil from 5-25 cm depths	-
TsoilB	Deep Soil Temperature	Celsius	Temperature of the soil below 25 cm	-
TSoilDepth	Soil Temperature Depth	cm	Measurement Depth for TsoilB, if no deep temp reported, this depth represents TsoilB	-
WTAverage	Water Table Average	cm	Average water table depth over the growing season, positive values represent water above the soil surface	-
WTMax	Water Table Max	cm	Max (highest) water table depth over the growing season, positive values represent water above the soil surface	-



WTMin	Water Table Min	cm	Minimum (lowest) water table depth over the growing season, positive values represent water above the soil surface	-
WTFluc	Water Table Fluctuation	cm	Fluctuation of the water table depth over the growing season (range between max and min)	-
SoilMoist	Soil Moisture	%	Soil Moisture percentage	-
SoilMostD	Soil Moisture Depth	cm	Depth the soil moisture was measured	-
Org	Organic Layer Depth	cm	Thickness of the organic layer	-
AL	Active Layer Depth	cm	Active layer depth at the time of measurement	-
Thaw	Thaw Depth	cm	Thaw depth	-
PfReg	Permafrost Region	C, D, S, N	Permafrost region where the study took place. Determined by mapping the coordinates over Brown et al. 1999 permafrost cover map	N: No permafrost, S: Sporadic/Isolated, D: Discontinuous, C: Continuous
PfConA	Permafrost Present	Y/N	Permafrost present in the top 2 meters, reported by the authors	Y: Yes, N: No
PfTh	Permafrost Thaw Present	Y/N	Permafrost thaw present, reported by the authors	Y: Yes, N: No
pH	pH	-	Soil pH	-
Sedge	Sedge	A, P, D	Sedge presence	A: Absent, P: Present, D: Dominant
Sphag	Sphagnum Cover	A, P, D	Sphagnum moss presence	A: Absent, P: Present, D: Dominant
Moss	Moss Cover	A, P, D	Non-sphagnum moss presence	A: Absent, P: Present, D: Dominant
Trees	Tree Cover	A, P, D	Tree presence	A: Absent, P: Present, D: Dominant
Shrubs	Shrub Cover	A, P, D	Shrub presence	A: Absent, P: Present, D: Dominant
Grid_T	Mean Annual Temperature (gridded)	Celcius	Gridded (0.5 by 0.5 degree) mean annual temperature from WorldClim2	-
TotalID	Unique site ID	-	Unique ID used as the random factor in mixed model analysis	-
CD_Pcp_An	Mean annual precipitation (gridded)	mm	Gridded (0.5 by 0.5 degree) mean annual precipitation from WorldClim2	-
BIOME	Biome	11, 6	Biome as defined by Olson et al. 2001 and the World Wildlife Fund	11: Tundra, 6: Boreal



### 2.3 Aquatic Methane Flux Dataset

360 The aquatic flux dataset includes ice-free season (~May-October depending on the location) and winter/ice-out fluxes  
and was compiled using data from studies published before February 2020. We identified new studies using 1) JStore™,  
Google Scholar™ and Web of Science™ searches with the terms (lake\* OR pond\*) AND (north\* OR boreal OR arctic OR  
sub-arctic) AND (methane OR CH<sub>4</sub> OR greenhouse gas\*); 2) references from published studies; and 3) contributions of  
unpublished data (n = 1). If multiple, yearly measurements were given for one site by the same study, we averaged the flux  
365 values (following the initial protocol taken by Wik et al. 2016a). If different studies reported fluxes from the same lake then  
these data were reported as separate entries. In instances where ice-free seasons fluxes and storage/ice-out fluxes were reported  
for the same lake, those data were entered on separate lines, but the number of lakes was designated as NA for the winter  
measurement as to not add to the total lake count. We defined sites based on reported average CH<sub>4</sub> fluxes. For example, some  
studies reported one average flux value for a group of lakes and this was considered one “site,” however, the number of lakes  
370 was noted. Studies that only reported CH<sub>4</sub> concentrations and not a flux estimate were not included.

Similar to the terrestrial dataset, the aquatic dataset focuses on small-scale measurement techniques that allow for  
flux estimates to be attributed to one specific land cover class. Therefore ice-free season diffusive fluxes included in this dataset  
were measured using dissolved CH<sub>4</sub> concentrations and modeling approaches (n = 254) or floating chambers (n = 181), while  
ebullitive fluxes were measured by bubble trap (n = 187) or floating chamber (n = 34). Diffusive modeling approaches include  
375 an estimate of the gas transfer coefficient, *k*. Gas transfer velocity estimates are commonly calculated using equations  
established by Cole and Caraco (1998). However, more recent efforts with EC systems, chambers, and either calculation or  
measurement of the near-surface turbulence that enables flux across the air-water interface indicates that fluxes using Cole and  
Caraco’s (1998) wind-based model of gas transfer velocities underestimate fluxes from non-sheltered waterbodies by a factor  
of two to four (Heiskanen et al. 2014; Mammarella et al. 2015; MacIntyre et al. 2020). Sheltered waterbodies, such as small  
380 lakes surrounded by trees, are an exception and can have reduced mean lake *k* values (Markfort et al. 2010). While we do not  
recalculate fluxes in this synthesis, we indicate which *k* calculations were used so that future studies and can easily identify  
and recalculate fluxes when required. Only a handful of eddy covariance (EC) measurements (n = 5) were included in the  
dataset. We included a limited number of EC measurements due to difficulties that most studies had in attributing the fluxes  
to lakes specifically. We classified all EC fluxes as diffusive fluxes as it is hard to separate between ebullition and diffusion  
385 within this measurement technique, however, for this reason, EC measurements were excluded from statistical analysis for  
ice-free season fluxes

We further delineated aquatic fluxes by transport pathway including ebullition (bubbles), diffusion (hydrodynamic  
flux), and winter storage/ice-out flux. Ebullition and diffusion measurements were averaged over the ice-free season to  
represent a mean daily flux estimate across a lake. In some cases, if measurements were only taken from one zone of the lake  
390 (i.e. just lake edge or just lake center) we averaged the fluxes and assumed whole-lake fluxes. Some studies only reported a  
seasonal ice-free flux estimate. If they also reported the number of days in the ice-free season, we then calculated the average



395 daily flux rate. Storage/ice-out flux includes the annual release of CH<sub>4</sub> that accumulates within and under the ice over the winter and includes estimates from ice bubble surveys (IBS). Our storage flux estimate does not include estimates of spring or fall circulation fluxes, wherein CH<sub>4</sub> that is stored in the deep portion of the water column is released upon season turnover of the water column (Karlsson et al. 2013; Sepulveda-Jauregui et al. 2015). We also include an estimate of the ice-free season ebullition and diffusive fluxes if provided by the authors or if the authors provided the number of ice-free days. Note that flux measurements that include the transport of CH<sub>4</sub> through littoral vascular plants were not included as aquatic fluxes, but as *Marsh* or *Tundra Wetland* fluxes within the terrestrial dataset.

400 In addition to aquatic CH<sub>4</sub> flux data, we also collected various site descriptors and categorical and continuous environmental variables (See Table 2 for detailed attribute information and additional variables not discussed here). For all sites we extracted information about the site name and location (latitude/longitude and country), the number of lakes for a reported flux estimate, sampling season (SEASON) and within lake sampling location (E.LOCATION), sampling pathway (PATHWAY), the general sampling dates (YEAR/MONTH) and the number of times sampled (D.DAYS/E.DAYS). When available, we added a column for the equation used to estimate the gas transfer velocity constant (*k*) using modeling approaches (K600\_EQ). Categorical variables included lake sediment type (BOTTOM), permafrost zone (PERMA.ZONE), presence of talik (TALIK), ecoregion (ECOREGION), and the original lake types outlined by Wik et al. (2016a) (LAKE.TYPE). BAWLD specific categorical variables include the overarching lake genesis type (TYPE), binned water body size (SIZE), and BAWLD land cover class (CLASS). When reported, we extracted the following continuous variables: surface area (SA), water body depth (DEPTH), water temperature (TEMP), dissolved organic carbon concentration (DOC), and pH. Gridded (0.5 by 0.5 410 degrees) climate variables including mean annual temperature (GRID\_T) and mean annual precipitation (CD\_Pcp\_An) were extracted from WorldClim2 (<http://www.worldclim.com/version2>).

**Table 2. Attribute information for the aquatic flux dataset.**

Column_Name	Variable_Name	Units_Info	Description	Controlled_Vocab
ID	Row ID	Numbers	Unique identifier for individual rows	
NUM	Study number	-	Number ID for independent publications	-
STUDY	Reference	-	Author name and year published	-
DATASET	Dataset	WIK, KUHN	Data entered originally included by Wik et al or new data entered by Kuhn et al.	WIK, KUHN
YEAR	Publishing year	-	Year the study was published	-
COUNTRY	Country	-	Country where the research took place	USA: United States, Canada, Russia, Sweden, Norway, Greenland, Finland
SITE	Lake name	-	Names of the lakes provided by the authors	-
NUMBER.LAKES	Number of Lakes	-	Number of lakes represented by the flux value presented	-
LAT	Latitude	Decimal Degrees	Coordinates given by the authors	-



LONG	Longitude	Decimal Degrees	Coordinates given by the authors	-
ECOREGION	Ecoclimate Region	CB,SB,ST,AT	Ecoclimatic regions as define by Olson et al. 2001	CB: Continental Boreal, SB: Subarctic boreal, ST: Subarctic tundra, AT: Arctic tundra
PERMA.ZONE	Permafrost Zone	N,S,D,C	Permafrost region where the study took place. Determined by mapping the coordinates over Brown et al. 1998 permafrost cover map	N: No permafrost, S: Sporadic/Isolated, D: Discontinuous, C: Continuous
LAKE.TYPE	Lake Type	BP,PP,GP,T,U	Lake type originally outlined by Wik et al. 2016	BP: Beaver Pond, PP: Peatland Pond, GP: Glacial/post-glacial, T: Thermokarst, U: Unspecified
BOTTOM	Bottom Sediment Type	M,O,P,Y,U	Sediment type as described by the authors	M: Minerogenic, O: Organic, P:Peat, Y:Yedoma, U:Unspecified
TALIK	Talik Present	Y,N	Is a talik present under the lake	Y: Yes, N: No
SA	Water body surface area	km <sup>2</sup>	Surface area reported by authors or determined by GIS if only the coordinates were given	-
DEPTH	Water body depth	meters	Mean lake depth reported by the authors; if mean was not reported, then the max was used	
SEASON	Sampling Days	Ice free, Winter	The time of the year the sampling took place. "Winter" includes winter ice surveys and ice-out measurements	Ice-free, Winter
YEAR.S	Sampling year(s)	year	The year or years the sampling took place	
MONTH	Sampling Months	Month names	The month or months the sampling took place	September, October, November, etc
PATHWAY	Method	D,E,S	The transport pathways measured	D:Diffusion, E: Ebullition, S:Storage, DE: Diffusion/Ebullition, DS: Diffusion/storage
D.METHOD	Diffusive measurement method	CH,WS,EC	The measurement method for diffusion	CH: Floating Chamber, WS: Water Sample, EC: Eddy Covariance
K600_EQ	K600 equation	-	Equation used to estimate the piston gas velocity coefficient (k) when calculating diffusive fluxes	-
K_REF	K600 reference	-	-	Citation for the k equation used
E.METHOD	Ebullition measurement method	BT, WS,IS	The measurement method for ebullition	BT: Bubble trap, CH: Chamber, IS: Ice survey
E.LOCATION	Ebullition measurement location	C,E,W	Location of the reported ebullition measurement	C: Center, E: Edge, W: Whole lake estimate



S.METHOD	Storage/ice out measurement method	BT,IS,WS	The measurement method for storage/Ice out	BT: Bubble trap, WS: Water sample, IS: Ice survey
D.DAYS	Diffusive measurement days	Days	Number of individual days diffusion was measured at the same lake	-
E.DAYS	Ebullition measurement days	Days	Total number of days a bubble trap was set to measure ebullition	-
LENGTH	Field sampling campaign length	Days	The duration of the field sampling campaign for each lake	-
CH4.D.FLUX	Diffusive fluxes	mg CH <sub>4</sub> m <sup>-2</sup> d <sup>-1</sup>	Mean daily diffusive fluxes	-
CH4.E.FLUX	Ebullitive fluxes	mg CH <sub>4</sub> m <sup>-2</sup> d <sup>-1</sup>	Mean daily ebullitive fluxes	-
SEASONAL.D	Seasonal Diffusive flux	grams m <sup>-2</sup> yr <sup>-1</sup>	Total diffusive fluxes over the season. Only included if the authors reported this value or the number of ice-free days	-
SEASONAL.E	Seasonal Ebullitive Fluxes	grams m <sup>-2</sup> yr <sup>-1</sup>	Total ebullitive fluxes over the season. Only included if the authors reported this value	-
SEASONAL.S	Seasonal Storage/ice-out	grams m <sup>-2</sup> yr <sup>-1</sup>	Below ice methane storage released upon ice-out in the spring	-
IBS	Ice Bubble Storage Fluxes	grams m <sup>-2</sup> yr <sup>-1</sup>	Ice-bubble methane storage released upon ice-out	-
TEMP	Water Temperature	Celsius	Water temperature as reported by the authors	-
DOC	Dissolved Organic Carbon	mg L <sup>-1</sup>	DOC concentrations as reported by the authors	-
PH	PH	-	Water column pH as reported by the authors	-
ICEFREE.DAYS	Number of Ice free days	Days	Number of ice-free days as reported by the authors	-
CLASS	Lake landcover class	LL, MGL, MPL, MYL, SGL, SPL, SYL	BAWLD land cover class type (includes size and lake origin type)	LL: Large Lakes, MGP: Midsize glacial, MPL: Midsize Peatland, MYL: Midsize Yedoma, SGL: Small glacial, SPL: Small peatland, SYL: Small Yedoma
SIZE	Categorical waterbody size	S, M, L	BAWLD land cover size class only	S: Small (<0.1km <sup>2</sup> ), M: Midsize (0.1-10 km <sup>2</sup> ), L (>10 km <sup>2</sup> )
TYPE	Land cover class type only	Y, P, G	BAWLD land cover lake origin type only	G- Glacial, P- Peatland, Y- Yedoma



CD_Pcp_An	Mean annual mm precipitation (gridded)		Gridded (0.5 by 0.5 degrees) mean annual precipitation from WorldClim2	-
BIOME	Biome	11, 6	Biome as defined by Olson et al. 2001	11: Tundra, 6: Biome
GRID_T	Mean annual temperature (gridded)	Celcius	Gridded (0.5 by 0.5 degrees) mean annual temperature from WorldClim2	
NOTES	Notes on the data	-	Miscellaneous notes on the data	

## 415 2.4 Statistics

All statistical analyses were performed in R statistical software (Version 1.1.383; [www.r-project.org](http://www.r-project.org)). We tested for significant relationships between log-transformed warm-season (terrestrial sites) or ice-free season (aquatic sites) average CH<sub>4</sub> fluxes and several covariates using a combination of linear regression and linear mixed-effects models when necessary (R Package 3.3.3; Lme4 Package; Bates et al. 2014). To include sites with CH<sub>4</sub> uptake or near zero fluxes we added a constant of 10 (terrestrial fluxes) or 1 (aquatic fluxes) before log transformation. Mixed-effects modeling was used when a given model included sites with multiple yearly measurements or if multiple studies reported fluxes from the same site (R “nmlr” package; Pinheiro et al., 2017). In these cases, site ID was included as a random effect in the analysis to help account for lack of independence across repeated measurements and to weight potential biases (Treat et al. 2018). Almost no studies in the terrestrial or aquatic datasets provided information on all of the variables, therefore, individual statistical analyses have different sample sizes, however, the same subset of data was used to select the best performing mixed models (n = 206 and n = 149 for the terrestrial and diffusive aquatic mixed models, respectively). The significance of individual predictor variables in the mixed models was evaluated using forward model selection. Model performance was conducted using size-corrected Akaike information criterion (AICc; “AICcmodavg” package; Mazerolle & Mazerolle, 2017), wherein a decrease in AICc by 2 or more as an indication of a superior model (as in Olefeldt et al. 2013 and Dieleman et al. 2020). All models were tested against each other and the null model. The null model only included the random effects. Non-parametric Tukey’s HSD post-hoc tests were performed to assess differences in median fluxes among sub-categories if the overall model was determined significant. All aquatic diffusive and ebullitive fluxes were analyzed separately. Eddy covariance flux estimates for aquatic ecosystems (n = 5) were not included in the statistical analysis since ebullitive and diffusive fluxes could not be partitioned. We modeled the temperature dependence (Q<sub>10</sub>) of CH<sub>4</sub> following Rasilo et al. (2015).

## 435 2.5 Limitations

Due to limitations of the studies where we extracted data from, some parts of the annual period are not considered in our dataset. Thus this dataset focuses on small-scale, surface-based spatial patterns in CH<sub>4</sub> fluxes associated with specific land

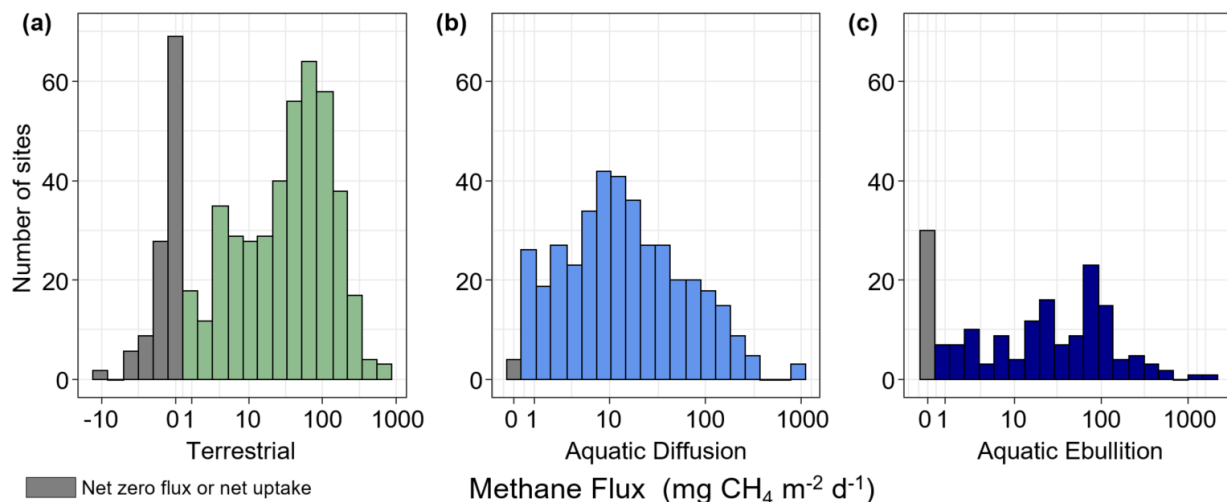


cover classes and does not represent temporal patterns in fluxes. For both terrestrial and aquatic datasets, we extracted data on the average CH<sub>4</sub> fluxes over warm periods or ice-free periods. While we do include an estimate of ice-out/winter fluxes from aquatic ecosystems, our dataset does not include autumnal turnover fluxes from aquatic ecosystems, which may represent a substantial portion of annual emissions (Fernández et al. 2014; Klaus et al. 2018). Nor do we include shoulder season or winter fluxes from terrestrial ecosystems, which can represent substantial components of the annual flux (Treat et al. 2018; Zona et al. 2016). Furthermore, our data extraction methods were not designed to assess inter-annual changes in fluxes as this dataset compiles the data of multiple studies over a large range of years (1986-2020). Despite data limitations, the datasets represent an important step forward regarding the spatial variability in fluxes among different land cover types.

### 3.0 Results

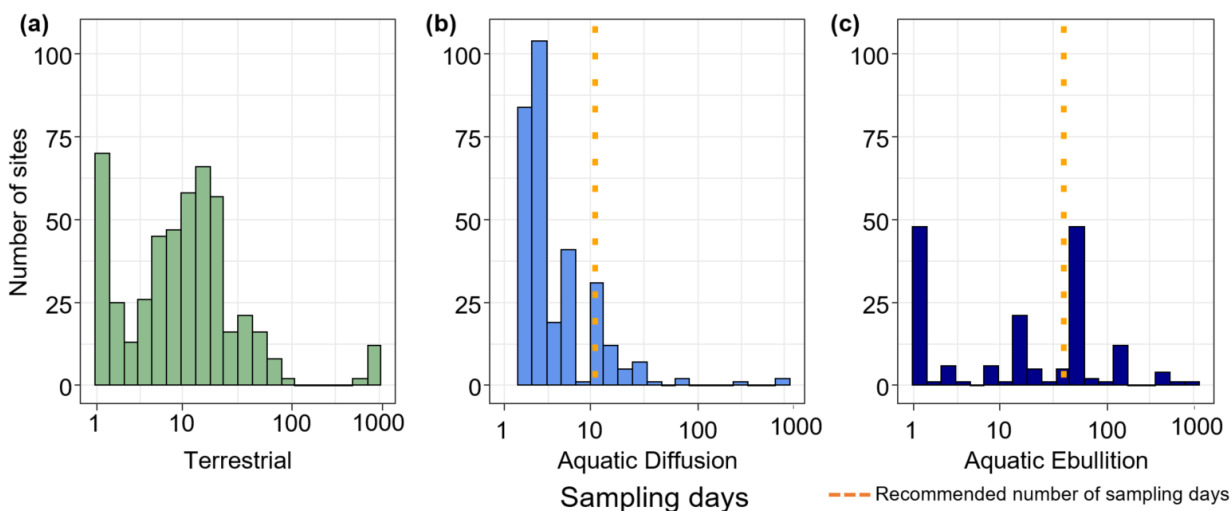
#### 3.1 Summary Statistics

In total, we extracted 555 site-year CH<sub>4</sub> estimates from terrestrial (wetland and non-wetland) ecosystems. The majority of reported fluxes (site-years) were from Canada and Greenland (34%), followed by Russia (27%), Alaska (25%), and Scandinavia (14%) (Fig. 1a). Terrestrial fluxes followed a bimodal distribution, split by net positive fluxes (82% of all reported fluxes) and net uptake or zero-emission (18% of all reported fluxes; Fig. 5a). The median number of measurement days per site-year flux for chamber measurements was 10 and the median number of collars per site measurement was five (Fig. 6a). Of the site-year fluxes reported from aquatic ecosystems, there were 441 diffusive estimates and 175 ebullitive ice-free season estimates, and 125 estimates of winter/ice-out fluxes (including storage, winter ebullition, ice bubble surveys, or a combination of the three). Aquatic sites were evenly distributed throughout the Boreal-Arctic region (Fig. 1b). Diffusive fluxes showed a unimodal distribution, while ebullition showed bimodal peaks near 100 and 0 mg CH<sub>4</sub> m<sup>-2</sup> d<sup>-1</sup> (Fig. 5b, 5c). The median number of measurement days per site-year flux was three and 15 for diffusion and ebullition, respectively (Fig. 6b; 6c). Winter/ice-out fluxes were reported as annual estimates and are shown in Table 5.



460

**Figure 5. Histograms of site-specific average CH<sub>4</sub> fluxes.** a) Terrestrial fluxes. b) Aquatic diffusive fluxes. c) Aquatic ebullitive fluxes. Grey bars represent net zero or net uptake fluxes.



465

**Figure 6. Histograms for the number of sampling days contributing to the average warm-season or ice-free season flux value.** a) Terrestrial flux sampling days. b) Aquatic diffusion flux sampling days. c) Aquatic ebullition sampling days. The orange dotted lines in panels b and c represent the number of recommended sampling days needed to arrive at a flux estimate within 20% accuracy (11 days for diffusion and 39 days for ebullition; Wik et al. 2016b).

470

### 3.2 Correlations with Terrestrial Fluxes

Of the continuous variables, water table ( $WT_{AV}$ ) and soil temperature ( $T_{SoilA}$  at 5-25 cm) were significantly and linearly correlated with  $CH_4$  ( $WT_{AV}$ :  $\chi^2 = 121$ ,  $P < 0.0001$ ,  $R^2_m = 0.28$ ,  $df = 380$ ;  $T_{SoilA}$ :  $\chi^2 = 54.6$ ,  $P < 0.0001$ ,  $R^2 = 0.21$ ,



df = 283) and gross primary productivity (GPP) was logarithmically correlated with CH<sub>4</sub> ( $\chi^2 = 5.8$ ,  $P = 0.016$ ,  $R^2m = 0.15$ ; df = 56; Fig. 7). However, given the relatively low sample size for GPP ( $n = 57$ ), we do not include GPP in mixed model analyses.

475 The temperature sensitivity ( $Q_{10}$ ) for all terrestrial emissions was 2.8 (SI Table 1). Of the categorical variables, there was no difference between the different permafrost zones ( $\chi^2 = 0.88$ ,  $P = 0.83$ , df = 539), but CH<sub>4</sub> fluxes were higher from sites without permafrost present in the top two meters ( $\chi^2 = 16.37$ ,  $P < 0.0001$ , df = 482; Fig. 8). For vegetation composition, sites dominated by shrubs had lower fluxes than those sites with shrubs present or absent ( $\chi^2 = 34.66$ ,  $P < 0.001$ , df = 2; Fig. 8). The strongest relationship between vegetation composition and CH<sub>4</sub> flux was emergent graminoid cover. Sites with dominant graminoid

480 composition had higher fluxes than sites where graminoids were present or absent ( $\chi^2 = 148.95$ ,  $P < 0.0001$ , df = 2; Fig. 8). The best explanatory model for terrestrial CH<sub>4</sub> emissions was an additive model that included site-level predictors of water table, soil temperature, and graminoid cover alongside the broader classification of land cover class ( $R^2m = 0.69$ ;  $P < 0.0001$ , df = 224; SI Table 2). There was no effect on model performance using interactive effects ( $\Delta AICc = 0.84$ ), however, the  $R^2m$  did increase to 0.73 (SI Table 2). Notably, on their own, individual models with just the site-level predictors or with just

485 land cover type explained close to the same amount of variation in CH<sub>4</sub> fluxes ( $R^2m = 0.55$  and  $0.54$ , respectively). Methane uptake fluxes, when analyzed separately, were positively correlated with thaw depth (i.e. more uptake with greater thaw depths;  $R^2m = 0.55$ ,  $\chi^2 = 19.61$ ,  $P < 0.0001$ , df = 22; SI Fig. 1). No other continuous variables were correlated with CH<sub>4</sub> uptake, however, sites, where shrubs were present, had significantly higher uptake than sites where shrubs were absent or dominant (Tukey PostHoc,  $P < 0.001$  for both, df = 2; SI Fig. 2).



490

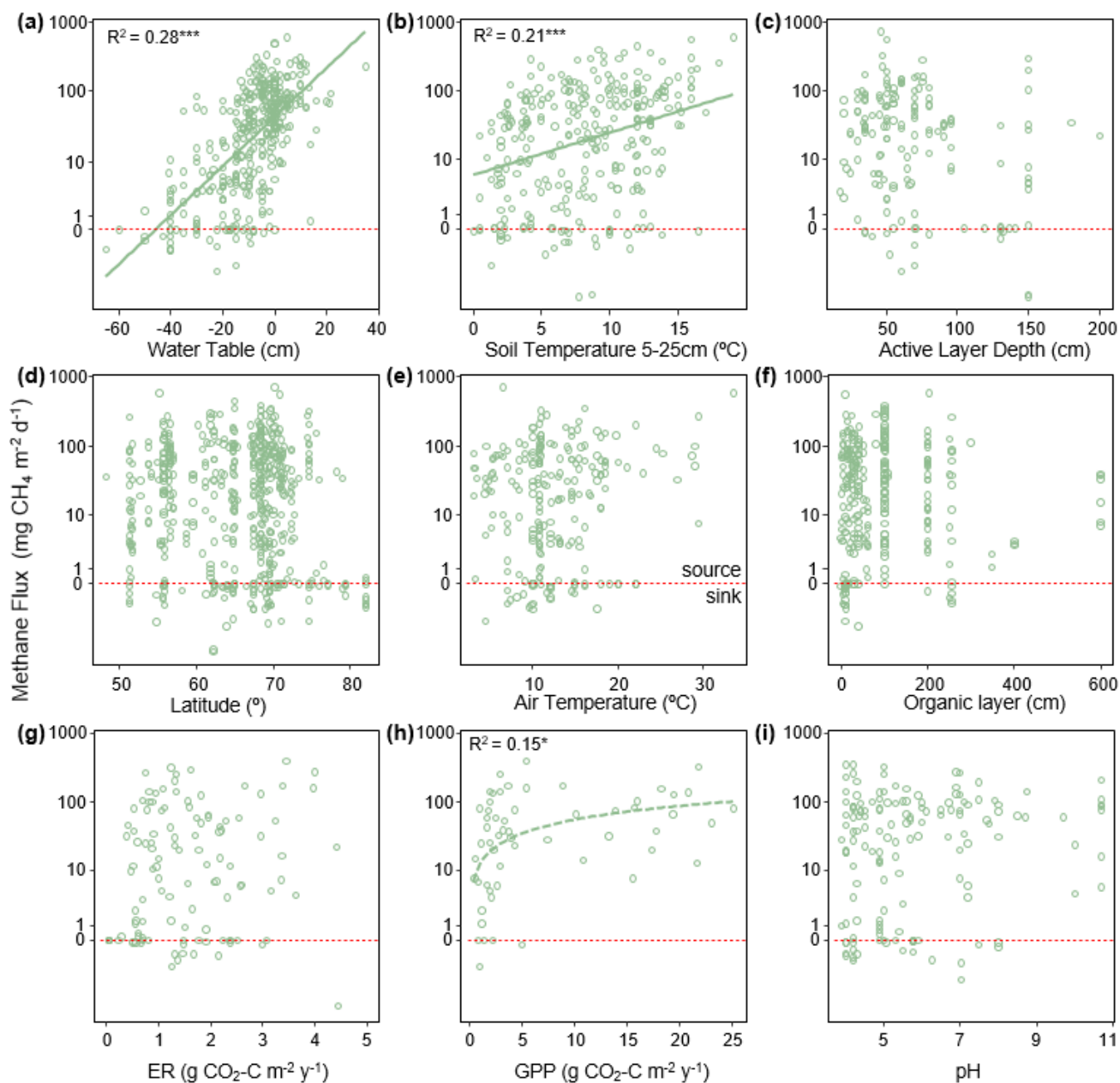
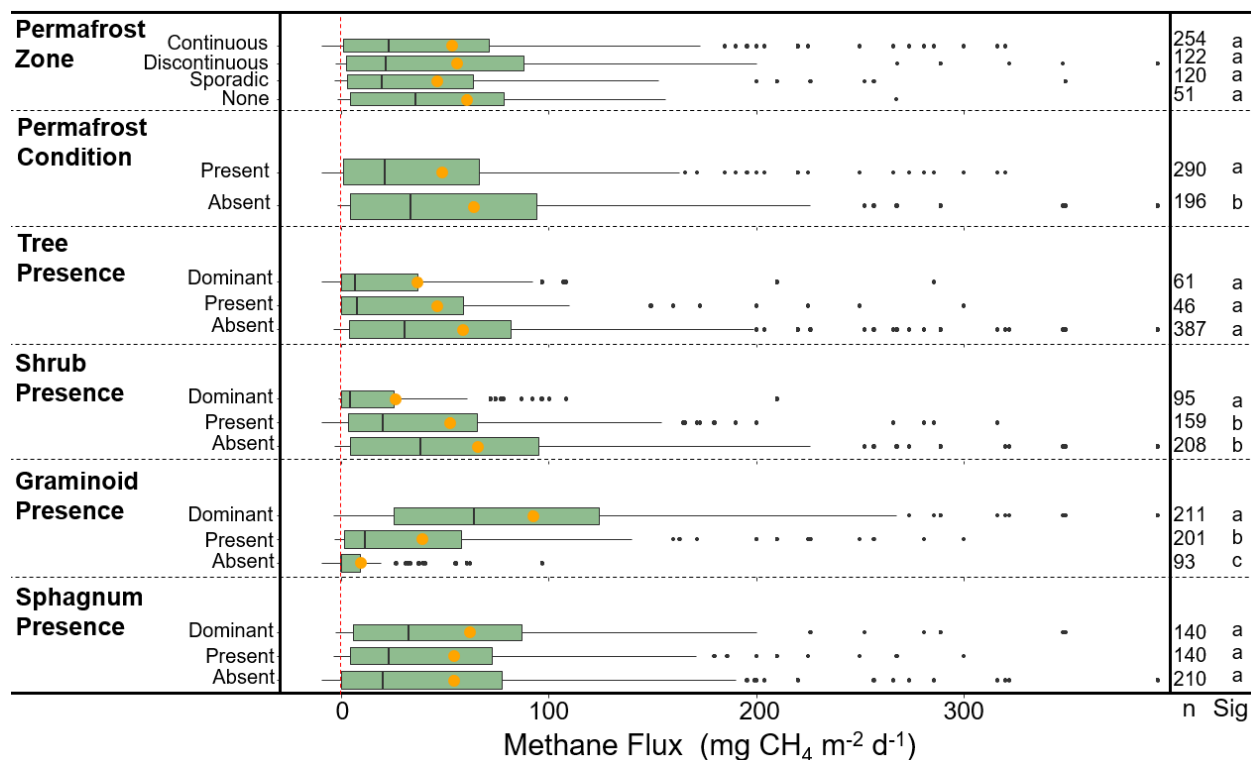


**Figure 7. Relationships between site-averaged warm-season CH<sub>4</sub> flux and environmental variables.** Environmental variables include water table, soil temperature at 2-25 cm depth, active layer depth, latitude, air temperature, organic layer thickness, ecosystem respiration (ER), gross primary productivity (GPP), and soil pH. Regression lines and R-square values are shown for significant relationships. Note the log scale. CH<sub>4</sub> flux was linearly related to water table and soil temperature and was logarithmically related to GPP (dotted line). Points below the red dotted line represent net uptake fluxes. \*  $P < 0.05$  \*\*  $P < 0.01$  \*\*\*  $P < 0.001$

495



500 **Figure 8. Warm-season CH<sub>4</sub> fluxes classified by categorical variables.** Orange circles represent mean flux values. The number of sites for each category is represented in the column to the right (n) and statistical differences among the categories are indicated by the letters (Sig). Permafrost zones are from Brown et al. 2002. Permafrost condition represents the presence of permafrost in the top 2 meters as reported by the authors. See text for definitions used to classify vegetation cover. Outlier fluxes greater than 380 are not shown.

505 There were significant differences in fluxes among the BAWLD terrestrial land cover classes ( $\chi^2 = 253.69, P < 0.001, df = 6$ ; Fig. 9a, Table 3). Median fluxes were highest from *Marshes, Tundra Wetlands, and Fens* (mean water table = +2, -0.4, and -6 cm, respectively). Median fluxes from *Bogs* were lower than the *Marshes, Tundra Wetlands, and Fens*, but higher than *Permafrost Bogs, Dry Tundra, and Boreal Forests*. *Permafrost Bogs* were the only wetland class that fell into the lowest emitting group of classes. However, the frozen and elevated nature of *Permafrost Bogs* typically leads to lower water table conditions more similar to *Dry Tundra* and *Boreal Forests* (mean water table = -22, -15, and -40 cm, respectively). However, it must be noted that in most *Boreal Forest* sites the water table is not in the top two meters, therefore water table is not commonly measured or reported. The mean water table depth presented here is likely an over estimate that represents wetter *Boreal Forest* sites that had measurable water tables in the top two meters. *Boreal Forest* ecosystems were the only class to have negative median CH<sub>4</sub> flux for the entire class (net uptake). *Permafrost Bogs* and *Dry Tundra* classes also included net uptake site-year CH<sub>4</sub> estimates (n= 17 and 31, respectively). One *Wetland Tundra* site in the Canadian High Arctic had net CH<sub>4</sub> uptake for one of the three years it was measured (Emmerton et al. 2014). Notably, the apparent temperature sensitivity



515 from the drier terrestrial sites (*Boreal Forest, Dry Tundra, and Permafrost Bogs*;  $Q_{10} = 3.7$ ) was higher than from the wet  
 terrestrial sites (*Marshes, Tundra Wetlands, Bogs, and Fens*;  $Q_{10} = 2.8$ ).

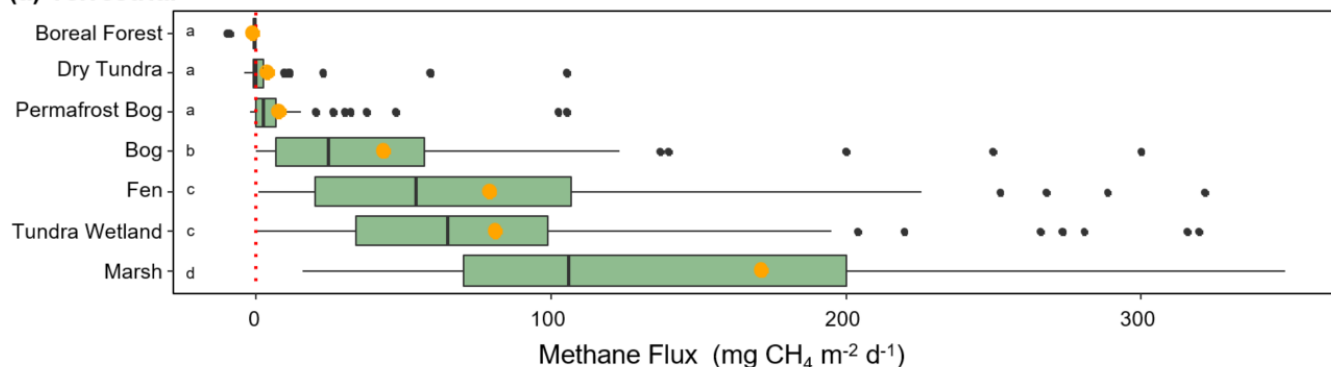
520 **Table 3. Characteristics of BAWLD terrestrial classes based on environmental variables.** The number of sites (site years) and  
 contributing studies are shown for each class. Also shown are the mean, median, and quartiles for site average  $CH_4$  flux, water table, soil  
 temperature between 5 and 25 cm (TSoilB), sedge cover, pH, ecosystem respiration (ER), and gross primary productivity (GPP). \*In some  
 cases one study contributed flux data for multiple classes.

		<b>Boreal Forest</b>	<b>Dry Tundra</b>	<b>Permafrost Bog</b>	<b>Bog</b>	<b>Fen</b>	<b>Tundra Wetland</b>	<b>Marsh</b>
<b>Sites</b>		30	63	81	87	109	109	33
<b>Studies*</b>		15	30	34	36	33	47	20
<b>CH<sub>4</sub></b>	Mean	-1.1	3.83	7.79	43.45	79.61	81.54	171.61
<b>Flux</b>	Median	-0.4	-0.01	2.32	24.55	54	65	106.00
<b>(mg CH<sub>4</sub> m<sup>-2</sup> d<sup>-1</sup>)</b>	25 <sup>th</sup>	-0.87	-1.09	0	6.92	20	34	70.50
	75 <sup>th</sup>	-0.17	2.4	6.9	57.35	107.20	99.30	200
<b>Water</b>	Mean	-38.37	-14.67	-22.16	-12.65	-5.98	-0.40	2
<b>Table</b>	Median	-42.50	-14.50	-20	-11	-5	0	0
<b>(cm)</b>	25 <sup>th</sup>	-50	-19.50	-37.25	-20	-10	-5	-3.5
	75 <sup>th</sup>	-25.3	-8.3	-10.3	-5	-1	4	5
	n	6	30	62	67	91	91	23
<b>TSoilB</b>	Mean	9.4	4.7	5	10.7	11.6	5.6	11.6
<b>(°C)</b>	Median	10	3.85	4.2	11.24	12	5	11
	25 <sup>th</sup>	8.8	2	2.5	9.2	9.5	3.6	8.8
	75 <sup>th</sup>	11	6.7	6.9	12.20	13.4	7.4	15
	n	14	20	53	51	60	59	17
<b>Average</b>	Dom	0%	17%	14%	23%	61%	61%	91%)
<b>Sedge Cover</b>	Pres	27%	59%	53%	49%	34%	38%	9%
	Absent	73%	28%	21%	28%	5%	1%	0%
	n	26	54	78	82	107	105	32
<b>pH</b>	Median	4.2	5.8	4.9	4.9	6.7	6.1	5.8

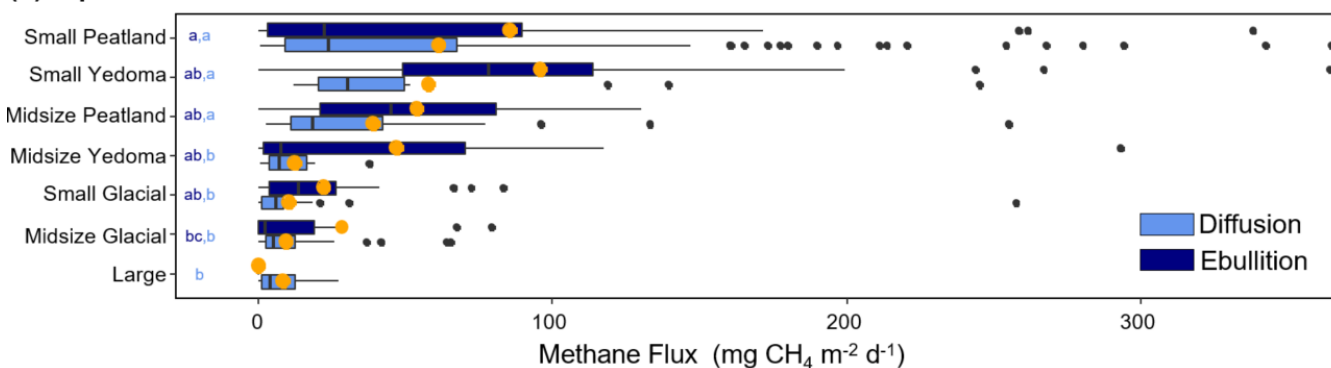


	n	9	12	11	29	42	25	10
<b>ER</b>	Median	2.3	1.5	1	1.6	1.93	1.4	3.25
<b>(g C m<sup>-2</sup> yr<sup>-1</sup>)</b>	n	6	18	55	20	14	27	5
<b>GPP</b>	Median	-	2.2	1.6	7.4	15.5	2.4	3.4
<b>(g C m<sup>-2</sup> yr<sup>-1</sup>)</b>	n	-	3	9	13	17	11	2

**(a) Terrestrial**



**(b) Aquatic**



525

**Figure 9. Relationship between methane flux and BAWLD land cover classes.** A) Terrestrial fluxes per each class. B) Aquatic fluxes including diffusion and ebullition per each class. Orange dots represent the arithmetic mean flux values and black lines represent median flux values. Boxes represent 25<sup>th</sup> and 75<sup>th</sup> percentiles. Outlier fluxes over 380 are not shown. The letters represent significant differences in fluxes among classes. Similar letters indicate no significant difference.

530 **3.3 Correlations with Aquatic Fluxes**

Diffusive CH<sub>4</sub> fluxes from aquatic ecosystems were negatively correlated with the continuous variables logged surface area ( $\chi^2 = 73.0, P < 0.0001, R^2_m = 0.20, df = 235$ ; Fig. 2.10a), logged waterbody depth ( $\chi^2 = 23.5, P < 0.0001, R^2_m = 0.09, df = 275$ ; Fig. 2.10b), latitude ( $F = 54.6, P < 0.0001, R^2 = 0.13, df = 361$ ; Fig. 2.10c), and positively correlated with DOC ( $F = 71.7, P < 0.0001, R^2 = 0.21, df = 261$ ; Fig. 2.10d) and water temperature ( $F = 57.2, P < 0.001, R^2 = 0.19, df = 236$ ; Fig.



535 2.10e). The apparent  $Q_{10}$  for diffusive emissions was 4.3 (Table A.2.1). Diffusive  $CH_4$  fluxes were highest from the sporadic  
permafrost zone ( $\chi^2 = 17.2$ ,  $P = 0.002$ ,  $df = 3$ ; Fig. 2.11). Furthermore, diffusive fluxes were significantly higher from small  
lakes compared to midsize and large lakes ( $\chi^2 = 30.5$ ,  $P < 0.0001$ ,  $df = 2$ ; Fig. 2.11) and from lakes with peaty/organic-rich  
sediments compared to lakes with *Yedoma* and *Glacial* sediment types ( $\chi^2 = 103.9$ ,  $P < 0.0001$ ,  $df = 2$ ; Fig. 2.11). The best  
explanatory model for diffusive  $CH_4$  fluxes was an additive model including an interaction between lake surface area  
540 (continuous) and type (i.e. overarching lake genesis) alongside water temperature as predictor variables ( $F = 14.9$ ,  $P < 0.0001$ ,  
 $adj.R^2 = 0.41$ ,  $df = 149$ ; Table A.2.3). Land cover class on its own explained 25% of the flux variation ( $F = 22.8$ ,  $P < 0.0001$ ,  
 $df = 149$ ).

Ebullitive  $CH_4$  fluxes from aquatic ecosystems were positively correlated with logged DOC ( $F = 12.25$ ,  $P = 0.0008$ ,  
 $adj.R^2 = 0.14$ ,  $df = 71$ ; Fig. 10d) negatively correlated with surface area ( $F = 13.88$ ,  $P = 0.0003$ ,  $adj.R^2 = 0.08$ ,  $df = 164$ ; Fig.  
545 10a) and latitude ( $F = 5.38$ ,  $P = 0.02$ ,  $adj.R^2 = 0.03$ ,  $df = 160$ ; Fig. 10c) and were weakly correlated with water temperature ( $F = 5.55$ ,  
 $P = 0.02$ ,  $adj.R^2 = 0.06$ ,  $df = 67$ ; Fig. 10e). The apparent  $Q_{10}$  for ebullitive emissions was 2.4 (SI Table 1). There was  
no apparent relationship with lake depth and ebullitive fluxes ( $F = 0.02$ ,  $P = 0.91$ ,  $df = 151$ ; Fig. 10b). There were no differences  
in ebullitive emissions between the permafrost zones with the exception of lower ebullitive emissions from the continuous  
zone compared to the sporadic zone (Tukey' HSD,  $P < 0.001$ ; Fig. 11). Similar to diffusive fluxes, ebullitive fluxes were  
550 higher from the small lake classes compared to midsize lakes (Wilcoxon Rank Sum,  $P = 0.0006$ , note that *Large lakes* did not  
have a large enough sample size ( $n=1$ ) to be included in the post-hoc analysis). Finally, ebullitive fluxes were similarly higher  
from *Peatland* and *Yedoma lakes* compared to *Glacial lakes* (Tukey' HSD,  $P = 0.006$  and  $0.001$ , respectively). The best  
explanatory model for ebullitive fluxes using a subset of the data with complete information for predictor variables of interest  
(i.e. SA, log.CH4.E.FLUX.plus1, SITE, CLASS, SIZE, DOC, TYPE, LAT, GRID\_T) included just water body surface area  
555 (continuous) as a predictor variable ( $F = 19.85$ ,  $P = 0.0001$ ,  $adj.R^2 = 0.21$ ,  $df = 68$ ).

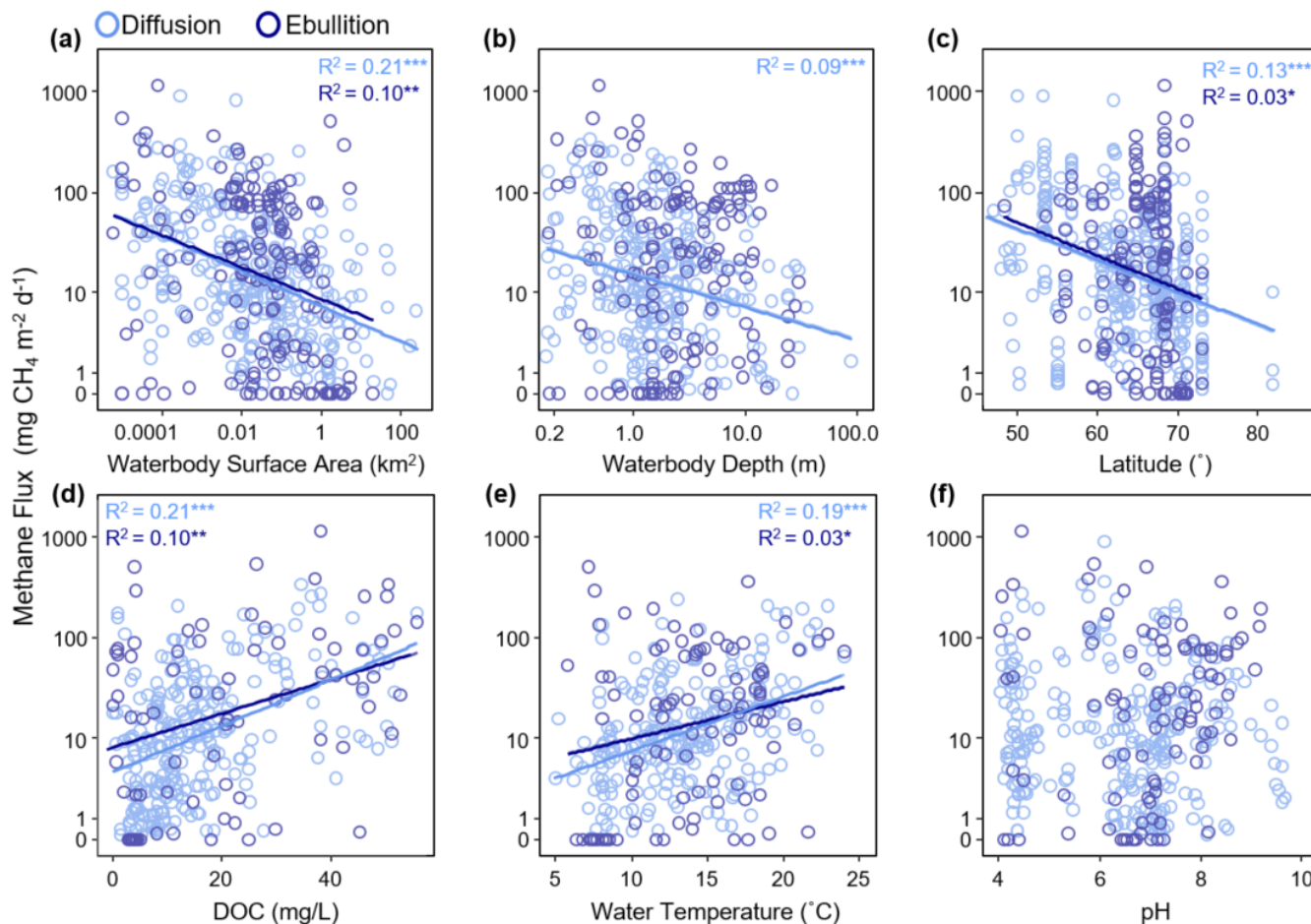
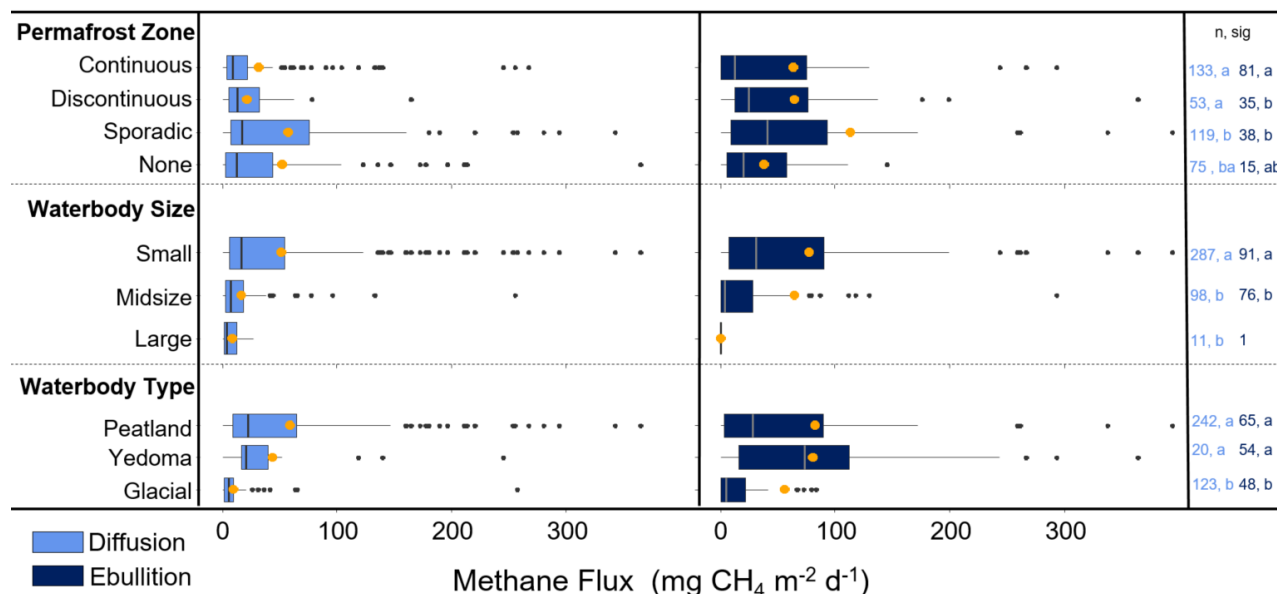


**Figure 10. Relationships between site-averaged ice-free diffusive and ebullitive CH<sub>4</sub> fluxes (note the log scale) and environmental variables.** Environmental variables include surface area, waterbody depth, latitude, dissolved organic carbon (DOC) concentration, water temperature, and pH. Regression lines and R-square values are shown for significant relationships. Log diffusive CH<sub>4</sub> flux was linearly related to surface area, depth, latitude, water temperature, and DOC. Log ebullitive fluxes were linearly related to surface area, latitude, DOC, and water temperature. \*  $P < 0.05$ . \*\*  $P < 0.01$ . \*\*\*  $P < 0.001$ .

560



565 **Figure 11. Ice-free season diffusion (left) and ebullitive (right) CH<sub>4</sub> fluxes as described by categorical variables.** Orange circles represent mean flux values. The number of sites for each category is represented in the column to the right (n) in the representative colors for diffusion (light blue) and ebullition (dark blue). The letters (Sig) indicate statistical differences among the categories. Lake Size represents binned surface areas for < 0.1 km<sup>2</sup> (Small), 0.1 – 10 km<sup>2</sup> (Midsized), and > 10 km<sup>2</sup> (Large). Lake Type represents the BAWLD classification of waterbody types including *Peatland*, *Yedoma*, and *Glacial lakes*. Fluxes higher than 380 are not shown.

570 There were clear differences in diffusive CH<sub>4</sub> fluxes among the aquatic class types, but few differences were observed for ebullitive fluxes. Diffusive fluxes were higher from the *Peatland* and *Yedoma lake* classes (both small and midsized), associated with organic-rich sediments, compared to mineral-rich glacial and large lakes ( $\chi^2 = 119.8$ ,  $P < 0.001$ ,  $df = 6$ ; Fig. 9b; Table 4). While ebullition fluxes appear to follow a similar trend to diffusive fluxes, the only significant difference was between *Small Yedoma lakes* and *Midsized Glacial lakes* (Tukey' HSD,  $P < 0.001$ ; Fig. 9b). However, the lack of statistical differences found for ebullition between lake classes may in part be due to fewer and more variable ebullition measurements compared to diffusion (Table 4). Reported winter ice-out emission estimates (including storage flux and Ice Bubble Survey (IBS) flux) were scarce in comparison to reported ice-free season emissions. *Small Glacial Lakes* and *Midsized Glacial Lakes* had the most reported winter ice-out emission estimates (n= 20 and 31, respectively). Average winter emissions (storage flux + IBS) generally were lower than annual estimates of ice-free diffusive and ebullitive emissions (Table 5); however, statistical tests were not performed across all of the classes due to low sample sizes from some of the classes. Winter ebullition estimates (i.e. direct ebullition emission to the atmosphere from seeps during the ice-cover winter season) were not included in winter emission sums because of the non-uniform spatial nature of these emission types (Sepulveda-Jauregui et al. 2015; Wik et al. 2016a), but are shown in Table 5. In the future, more estimates of winter emissions from aquatic systems are needed to more accurately estimate total annual emissions.



585

590

**Table 4. Characteristics of the BAWLD aquatic classes based on CH<sub>4</sub> and environmental variables.** The number of sites and contributing studies are shown for each class and flux pathway. Also shown are the mean, median, and quartiles for site average diffusive and ebullitive CH<sub>4</sub> flux, waterbody surface area, water body depth, and dissolved organic carbon concentrations (DOC). \*In some cases one study contributed flux data for multiple classes and pathway types. One ebullition outlier point (flux = 1815 mg CH<sub>4</sub> m<sup>2</sup> d<sup>-1</sup>) was excluded from the *Midsize Glacial* class as it was influenced by beaver activity (Sepulveda-Jauregui et al. 2015).

		Large Lakes	Midsize Glacial	Small Glacial	Midsize Yedoma	Midsize Peatland	Small Peatland	Small Yedoma
<b>Studies*</b>		7	23	15	18	13	39	6
<b>Lakes* D</b>		168	447	52	7	43	400	17
<b>Lakes* E</b>		1	34	19	38	26	50	34
<b>Diffusive</b>	Mean	8.6	9.5	10.5	12.3	39.1	61.2	57.8
<b>CH<sub>4</sub> Flux (mg CH<sub>4</sub> m<sup>-2</sup> d<sup>-1</sup>)</b>	Med	3.8	5.1	5.8	6.8	18.4	16.4	30.5
	25 <sup>th</sup>	1.1	2.4	1.1	3.4	11.0	9.1	20.5
	75 <sup>th</sup>	12.2	12.3	8.6	16.5	42	101.6	49.7
	n	11	68	55	6	24	218	14
<b>Ebullitive</b>	Mean	0	24.12	22.1	46.8	54.0	85.6	95.9
<b>CH<sub>4</sub> Flux (mg CH<sub>4</sub> m<sup>-2</sup> d<sup>-1</sup>)</b>	Med	0	1.65	13.3	7.5	45.1	22.5	78.3
	25 <sup>th</sup>	0	0	3.4	1.8	20.8	3.2	49.1
	75 <sup>th</sup>	0	15.4	26.5	70.1	80.5	89.4	113.8
	n	1	35	19	15	7	57	33
<b>Surface</b>	Mean	52.9	1.2	0.03	1.2	1.03	0.0123	0.03
<b>Area (km<sup>2</sup>)</b>	Med	42.6	0.5	0.02	0.56	0.25	0.002	0.02
	25 <sup>th</sup>	17	0.2	0.01	0.32	0.13	0.0001	0.008
	75 <sup>th</sup>	48.4	1.4	0.05	1.2	0.48	0.01	0.04
	n	16	106	61	16	24	201	48
<b>Depth (m)</b>	Mean	21.4	7.7	4.6	4.7	2.0	1.2	4.9
	Med	15.6	4.6	3.15	2.8	1.4	1	4.3
	25 <sup>th</sup>	9	1.8	2.5	2.1	1	0.5	2.6
	75 <sup>th</sup>	26.5	11.4	6.7	4.8	1.6	1.7	6
	n	13	90	46	16	17	178	49
<b>DOC</b>	Mean	7.7	7.3	13.4	7.8	12.0	20.3	23.2



(mg L <sup>-1</sup> )	Med	8	4.6	7.6	4.7	10.6	16.6	16.3
	25 <sup>th</sup>	5.9	3.2	4.2	4.0	8.4	11.0	14.9
	75 <sup>th</sup>	8.1	8.1	11.3	4.8	11.3	25.8	35.3
	n	11	62	33	8	17	162	11

595 **Table 5. Winter fluxes, including storage, ice bubble storage (IBS), and winter ebullition for each class type.** Annual estimates of ice-free diffusion and ebullition are included for comparison. \*\* Winter ebullition from constant seeps not included in sum winter/ice-out emissions.

Class	Annual Flux (g CH <sub>4</sub> m <sup>-2</sup> yr <sup>-1</sup> )	Storage	Ice Bubble Storage	Winter Ebullition (Seeps)**	Ice-free Diffusion	Ice-free Ebullition
<b>Small Peatland Lakes</b>	Mean (n)	1.3 (4)	1.3 (4)	9.5 (4)	10.50 (97)	12.61 (38)
	Median	1.5	1.5	2.3	4.50	5.50
	25 <sup>th</sup>	0.8	0.8	1.7	1.62	1.26
	75 <sup>th</sup>	1.9	1.9	10.1	12.10	14.33
<b>Small Glacial Lakes</b>	Mean (n)	1.3 (14)	1.3 (14)	1.1 (6)	0.78 (46)	4.72 (8)
	Median	0.5	0.5	1.2	0.70	4.95
	25 <sup>th</sup>	0.1	0.1	0.7	0.13	3.98
	75 <sup>th</sup>	2.6	2.6	0.6	1.14	7.52
<b>Small Yedoma Lakes</b>	Mean (n)	0.4 (6)	0.4 (6)	2.3 (10)	6.18 (11)	11.14 (16)
	Median	0	0	1.1	3.20	3.70
	25 <sup>th</sup>	0	0	0.4	2.70	1.50
	75 <sup>th</sup>	0.5	0.5	3.8	5.70	14.55
<b>Midsize Peatland Lakes</b>	Mean (n)	0.9 (1)	0.9 (1)	1 (1)	4.02(6)	6.47 (4)
	Median	-	-	-	2.85	6.04
	25 <sup>th</sup>	-	-	-	1.65	3.85
	75 <sup>th</sup>	-	-	-	5.63	8.66
<b>Midsize Glacial Lakes</b>	Mean (n)	0.3 (19)	0.3 (19)	0.4 (12)	1.59 (54)	3.37(21)
	Median	0	0	0.3	0.6	0.92
	25 <sup>th</sup>	0	0	0.1	0.26	0.35
	75 <sup>th</sup>	1.7	1.7	0.5	1.41	1.7
<b>Midsize Yedoma Lakes</b>	Mean (n)	1.2 (3)	1.2 (3)	0.2 (3)	1.71 (5)	6.12 (5)



	Median	0.6	0.6	0.2	1.10	2.10
	25 <sup>th</sup>	0.5	0.5	0.15	0.50	0.70
	75 <sup>th</sup>	1.7	1.7	0.25	2.00	11.80
<b>Large Lakes</b>	Mean (n)	0 (4)	0 (4)	-	1.38 (9)	-
	Median	0	0	-	0.8	-
	25 <sup>th</sup>	0	0	-	0.25	-
	75 <sup>th</sup>	0	0	-	1.3	-

### 3.4 Joint Analysis of Terrestrial and Aquatic Fluxes

We performed joint analysis of fluxes from both the aquatic and terrestrial datasets with regional predictor variables (Class, MAAT, MAP, Permafrost Zone, and Biome) using mixed models to assess the potential for universal drivers across all Boreal-Arctic ecosystems. The best model included Class and MAAT ( $\chi^2 = 345.6$ ,  $P < 0.0001$ ,  $R^2_m = 0.47$ ,  $df = 18$ : SI Table 4). However, Class alone explained 44% of the variation in fluxes (compared to 47% in the best model; SI Table 4), suggesting that ecosystem classification based on CH<sub>4</sub> emitting characteristics, alongside corresponding spatial extent, is one of the most important variables to consider when scaling CH<sub>4</sub> fluxes across the Boreal-Arctic region.

## 4.0 Discussion

### 4.1 Flux Variation Largely Explained by Land Cover Classes

In this review, we assessed the controls on CH<sub>4</sub> emissions from 189 studies across terrestrial and aquatic ecosystems in the Boreal-Arctic region. A central component to this study was the inclusion of new land cover classes split by CH<sub>4</sub>-emitting characteristics common across terrestrial and aquatic ecosystems, respectively. Terrestrial classes were split by permafrost conditions and hydrology (and vegetation and nutrient conditions therein) whereas aquatic classes were split by size and lake genesis (i.e. type). We found that much of the observed CH<sub>4</sub> flux variability from terrestrial and aquatic ecosystems could be explained by this land cover classification system (Fig. 9). When modeling fluxes for both aquatic and terrestrial ecosystems together with regional-level predictors (variables assigned to sites based on the gridded product including Biome, Permafrost Zone, MAAT, and MAP) land cover class explained most of the variation (44%) with significant, but small contributions in explained variation from gridded MAAT (3% of 47% total variation explained; SI Table 2). This suggests that differences in land cover classes are the most important consideration for estimating CH<sub>4</sub> flux at this scale, with some influence of MAAT.

For terrestrial fluxes alone, land cover class as a predictor variable explained 55% of the flux variation. Site-level predictors, including water table, temperature, and vegetation conditions explained 54% of the variation in the fluxes when analysed separately. The best model for terrestrial fluxes included these site-level variables and land cover class and explained 69-73% of the variation (depending on additive or interactive effects; SI Table 2). This model likely performed better than land cover class on its own because the extra information added from the continuous soil temperature and water table variables



captured the variation in these conditions within each class. While permafrost presence came out as a non-significant term in our best model (SI Table 2), the effects of permafrost presence and absence, including confounding temperature effects, were already intertwined into the land cover classes.

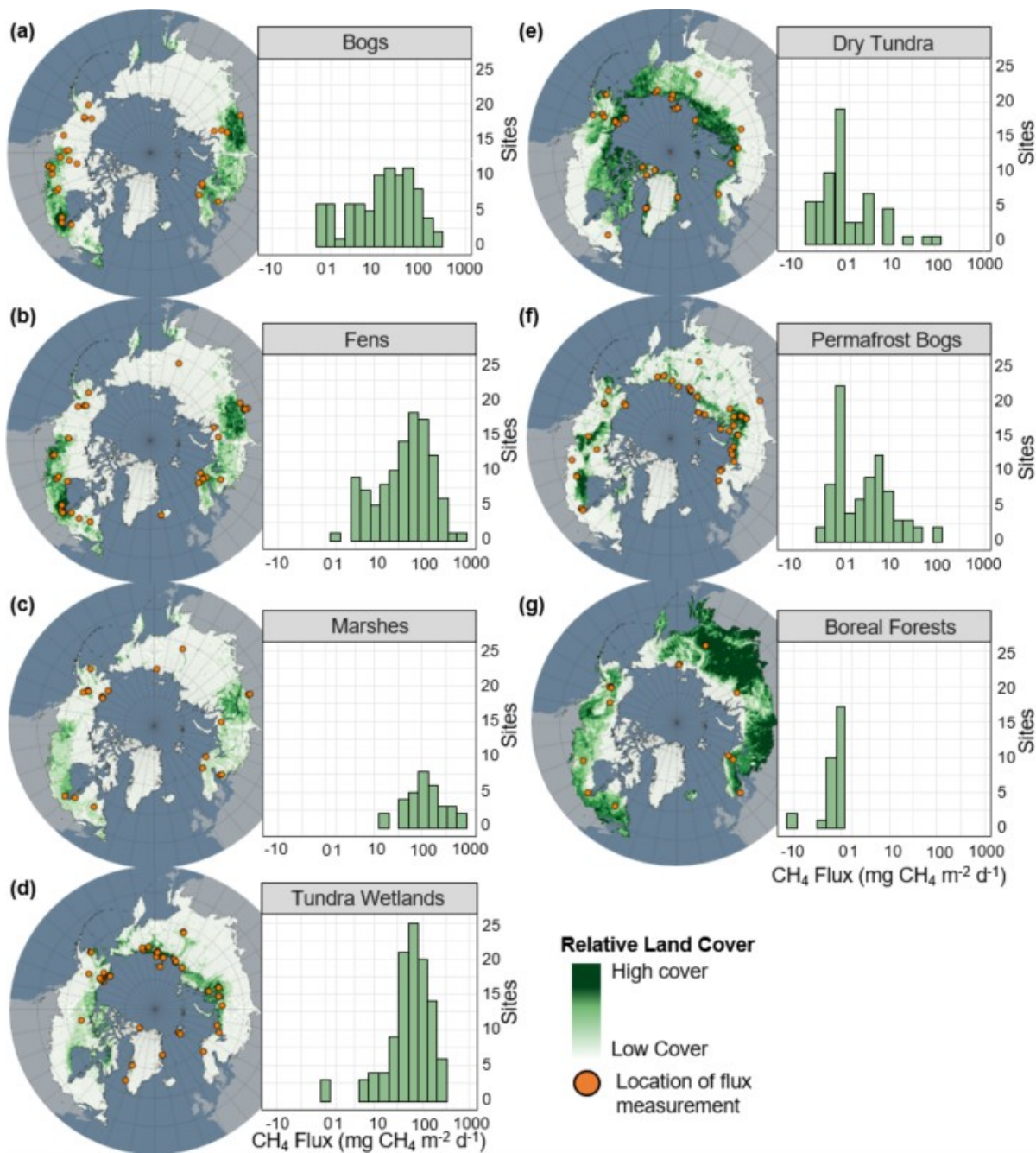
For aquatic ecosystems, the best models for diffusive and ebullitive fluxes contained different predictor variables. The best model for diffusive fluxes explained 41% of CH<sub>4</sub> flux variability and included an interactive effect between surface area and lake type (*Peatland*, *Yedoma*, and *Glacial*) and water temperature. Land cover classes (i.e. lake types split by small and midsize categorical sizes) did not come out as significant in this model because the continuous variable of surface area captures the size variation within each lake type. However, land cover class modeled on its own explained 25% of the flux variation. The significant effect of surface area is consistent with previous global synthesis efforts that found small water bodies tend to have higher CH<sub>4</sub> fluxes likely due to the compounding effects of higher substrate availability and warmer temperatures compared to larger water bodies (Holgerson and Raymond, 2016; DelSontro et al. 2018). Notably, previous synthesis efforts also found that water body depth was a significant predictor variable of diffusive fluxes (Wik et al. 2016a, Li et al. 2020). While depth did not come out as significant in our model, the effect of waterbody depth is taken into account with the lake types. For example, we found diffusive fluxes are typically higher from *Peatland lake* types compared to *Glacial lakes*, which have average depths of 1.6 meters and 6.7 meters, respectively. Waterbody depth is also an important factor contributing to water body temperature (i.e. warmer waters in shallower water bodies), thus the effect of water body depth may also be confounded with that of the temperature variable.

The best model for ebullition contained waterbody surface area as a predictor and explained 21% of the variation in the fluxes. Previous synthesis efforts have linked ebullition fluxes to both temperature (Aben et al. 2017) and waterbody depth (Wik et al. 2016a). The weak or absent relation with temperature and depth here is not surprising especially given the broad depth range of the lakes evaluated, nor contradicts the previously observed relationships, because it is likely that the temperature and depth influence is clearer over time and space, respectively, in each specific system. In this dataset, such patterns may be masked by differences in measurement strategies (i.e. number of measurements per season or measurement distributions over the lake) or among overall system characteristics. It is also possible the effects of depth are confounded with surface area as the two metrics are highly correlated (SI Fig. 5). While this dataset represents one of the largest collections of ebullitive emissions from northern lakes so far, this emission pathway is still largely underrepresented and waterbody depth and temperature are not always reported with the flux estimates. Furthermore, we collected information on surface water temperature for this dataset because it was the most widely available temperature metric. Sediment temperature is a better metric to collect in hand with ebullition due to production and transport directly from the sediments (Aben et al. 2017; Wik et al. 2013). Future studies should work to report sediment temperature and water column temperature alongside their flux measurements.

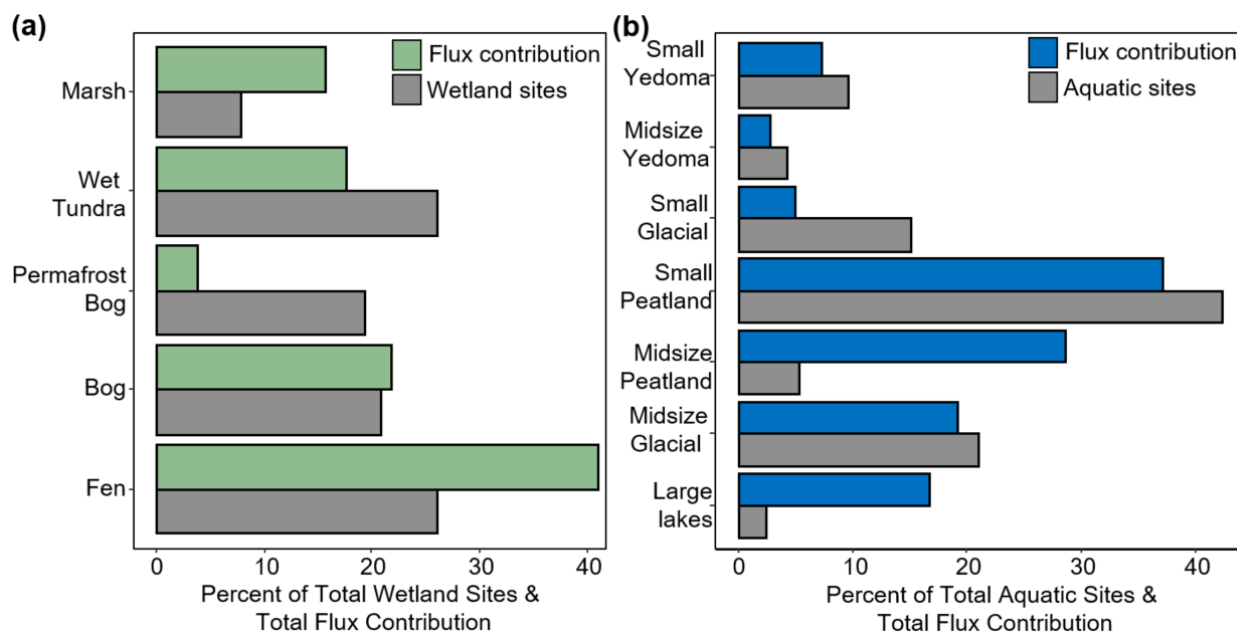


#### 4.2 Directions for Future Research

655 While our small-scale, surface CH<sub>4</sub> flux datasets for northern ecosystems are the most extensive datasets compiled to date for the Boreal-Arctic region, we identified key gaps in the data and areas of improvement that future studies should focus on. While the geographical gaps represented in Figure 1a suggest widespread geographic under-representation of terrestrial ecosystems, especially across central Russia and the Canadian Territories of Nunavut and Northwest Territories, these regions are comprised primarily of *Boreal Forest* and *Dry Tundra* ecosystems, respectively (Fig. 12e, 12g). Study sites for many of  
660 the other land cover types, for example, *Bogs* and *Fens*, were relatively well distributed across the Boreal and Arctic region (Fig. 12a, 12b). However, to assess how well or poorly represented a land cover class is, class area and flux magnitude must also be considered (Fig. 13a). For example, *Fens* are a high-emitting land cover class and are spatially abundant, leading to a high total flux contribution across the study region (~41%, Fig. 13a), however, the relative number of *Fen* sites represented in the available literature is not proportional to the total flux contribution (~26%). This, alongside the large spread of reported  
665 flux magnitudes (Fig. 9a), suggests future studies should focus on *Fens* to better constrain the flux magnitude. Conversely, *Permafrost Bogs* are low contributors to the total wetland flux (~4%) and sites are well represented throughout the literature (~19%), suggesting fewer direct flux measurements are needed from these ecosystems.



670 **Figure 12. Geographical distribution and flux frequencies and for each terrestrial class.** Relative land cover for each type is represented in green on the map. Site locations are represented by orange circles. Note the log scale for CH<sub>4</sub> flux. Land cover distributions from Olefeldt et al. 2021. Histograms of non-transformed flux data can be found in the SI Fig. 3.



675 **Figure 13. Relative total flux contribution (mean flux\*total class area) for each land cover shown with the relative contribution of flux measurements for each class. A) Wetland classes. B) Aquatic classes. The bars represent the percent of total flux contribution and percent of reported flux sites for each class. Aquatic flux contributions represent average ebullition + average diffusion fluxes.**

For aquatic ecosystems, there are key data gaps in geography and flux pathway representation with relatively few measurements of ebullition and ice-out fluxes compared to diffusive fluxes. Geographically there are very few flux measurements from lakes in the western Canadian Shield (Fig. 1b), despite this region containing the most lakes per unit area throughout the north (Messenger et al. 2016). This data gap is further highlighted by very few flux estimates from *Large lakes* and *Midsize-Glacial lakes*, which are numerous throughout the western Canadian Shield (Fig. 14a, 14d). Notably, *Large lakes* are the least represented of all of the aquatic classes (~2.4% of measurements), but could potentially contribute ~17% of the total flux, mostly from diffusive emissions. Interestingly, while *Small Peatland Lakes* are well represented (~42% of measurements and 37% of potential total flux contribution), *Midsize Peatland lakes* are under-represented (~5% of measurements) compared to their estimated flux contribution (~28%). Thus, *Large Lakes* and *Midsize Peatland Lakes* may be important focal points for future research however; more empirical scaling-based uncertainty analyses should be explored.

680  
685

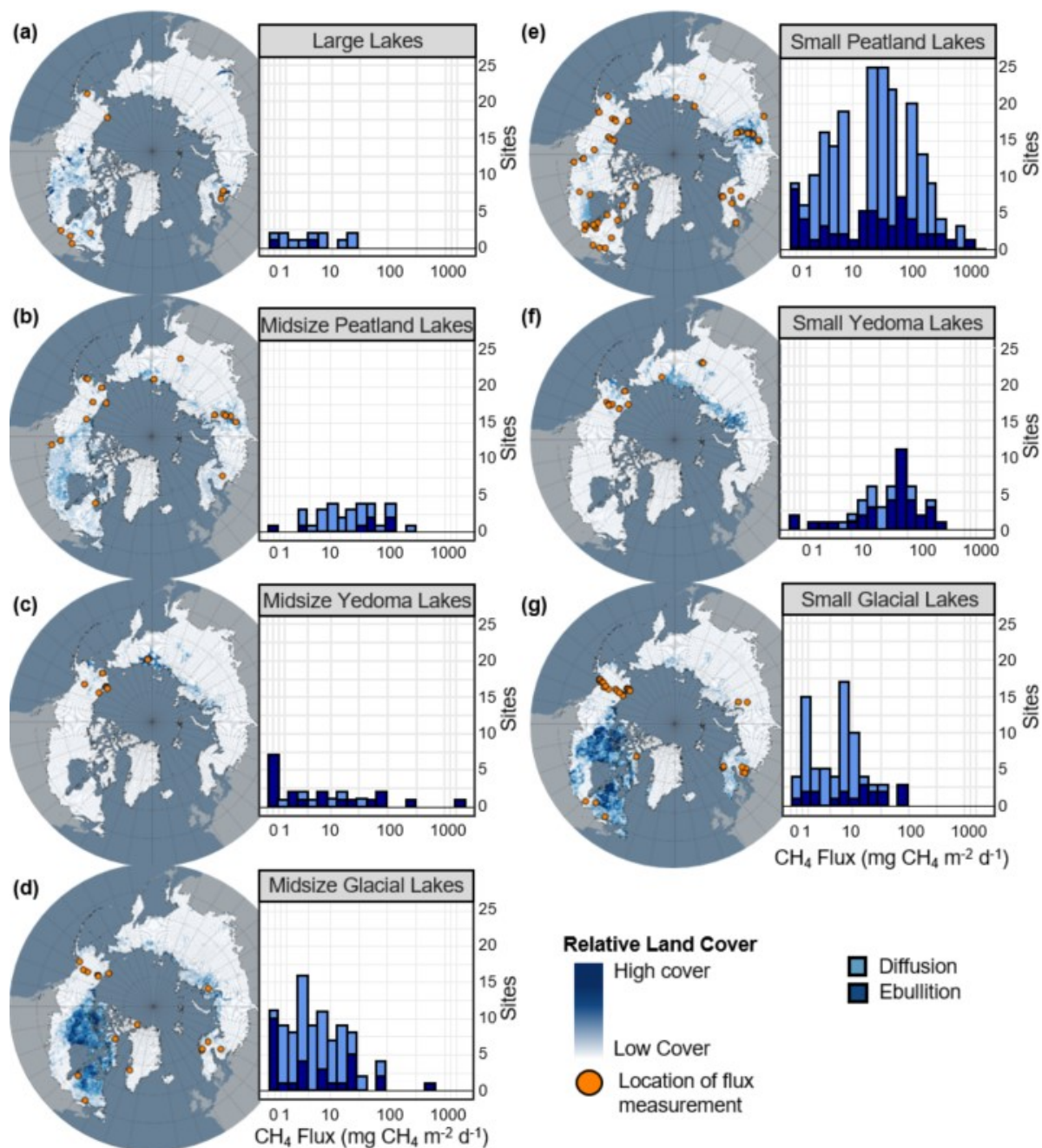


**Figure 14. Flux frequencies and geographical distribution for each aquatic class.** Relative land cover for each class type is represented in blue on the map. Site locations are represented by orange circles. Note the log scale for CH<sub>4</sub> flux. Land cover distributions from Olefeldt et al. 2021. Histograms of non-transformed flux data are shown in SI Fig. 4.

690

There are fewer ebullition measurements compared to diffusive flux measurements from aquatic ecosystems (21% and 79% of ice-free fluxes, respectively). Average ebullitive fluxes were greater than diffusive estimates for all of the land



cover classes except *Large Lakes* (Fig. 7b), and thus represent an important component of total CH<sub>4</sub> fluxes from these systems, however, none of the models performed in this study could explain a large amount of the variation in ebullitive fluxes. More ebullition measurements, across all the land cover classes, will help to constrain our understanding of CH<sub>4</sub> transport mechanisms and drivers. However, it is important to note that more representative ice-free season flux estimates are needed for both ebullition and diffusion. Wik et al (2016b) suggest that ~11 diffusive day flux measurements and ~39 ebullition day flux measurements are required to calculate a mean ice-free flux estimate within 20% of the true value. 86% of diffusive estimates were under the recommended 11-day mark and 58% of ebullition estimates were below the recommended 39-day mark (Fig. 5b, 5c). Jansen et al. (2020) posit that an even higher frequency of sampling is required (14-22 days and 135 days for diffusion and ebullition, respectively). Under-sampling potentially reduces the accuracy of mean CH<sub>4</sub> flux estimates leading to the relatively poor fitness and explanatory power of the aquatic regression analysis in this study compared to the terrestrial models' performances. This is especially true for ebullitive emissions, which were poorly explained by the reported predictor variables available for this dataset. Calculation of mean ice-free fluxes from a greater number of flux measurements is an important step forward towards better constraining CH<sub>4</sub> fluxes from aquatic ecosystems. Finally, there are very few flux estimates for lakes over the shoulder seasons and winter/ice-out compared to the ice-free season (Table 5). While shoulder season flux estimates, including autumnal turnover, were not included in this dataset, winter/ice-out measurements make up only 7% of all aquatic flux measurements collected. Winter/ice-out emissions could potentially contribute a significant portion of annual fluxes from aquatic ecosystems (Karlsson et al. 2013; Sepulveda-Jauregui et al. 2014) and therefore represent an important gap in CH<sub>4</sub> flux data.

## 710 5.0 Conclusions

Methane fluxes from northern ecosystems represent an important component of the global CH<sub>4</sub> cycle (Saunois et al. 2020). BAWLD-CH<sub>4</sub> is a comprehensive flux dataset that uniquely represents flux data from both terrestrial and aquatic ecosystems across the Boreal-Arctic region. BAWLD-CH<sub>4</sub> has many potential applications including benchmarking for process-based models, empirical scaling models and informing future research directions. Importantly, we show that land cover classes, split CH<sub>4</sub>-emitting ecosystem characteristics, is a significant flux predictor variable across terrestrial and aquatic ecosystems and we suggest that future studies should scale CH<sub>4</sub> emissions based on CH<sub>4</sub> -emitting land cover characteristics. We show that while land cover class explains most of the flux variation for wetland and aquatic ecosystems when analyzed jointly, both types of classes are somewhat sensitive to MAAT, which has important implications for future scaling efforts. Finally, we found that a higher percentage of terrestrial CH<sub>4</sub> fluxes could be explained by land cover class and site-level variables than for diffusive and ebullitive fluxes from aquatic ecosystems (73% vs 41% and 21%, respectively). Under-sampling of aquatic ecosystems is likely responsible for the lower explained variation observed in our models compared to terrestrial ecosystems. Future studies should increase the number of sampling days for both diffusive and ebullitive fluxes from aquatic ecosystems to arrive at more representative ice-free flux estimates and total CH<sub>4</sub> emissions from the Boreal-Arctic region.



## 725 6.0 Data Availability

The BAWLD-CH<sub>4</sub> flux dataset is available for download at the Arctic Data Center (<https://doi.org/10.18739/A27H1DN5S>).  
The companion land cover spatial data set is also available at the Arctic Data Center (<https://doi.org/10.18739/A2C824F9X>).

## Author Contributions

M.A.K. and D.O. conceived of the land cover classifications and project idea. D.O., D.M., P.C., and M.T. contributed to the original wetland flux dataset and conceptual ideas updated in this work. R.K.V., D.B., S.M., and K.W.A. contributed to the original lake flux dataset and ideas updated in this work. M.A.K. compiled and updated the flux databases, analyzed the data, and created the figures. M.A.K. wrote the manuscript. All authors contributed to data interpretation and commented on and improved the manuscript.

## Competing Interests

735 The authors declare that they have no conflict of interest.

## Acknowledgments

The Permafrost Carbon Network provided coordination support, and is funded by the NSF PLR Arctic System Science Research Networking Activities (RNA) Permafrost Carbon Network: Synthesizing Flux Observations for Benchmarking Model Projections of Permafrost Carbon Exchange, Grant # 1931333 (2019-2023). We thank Claire Treat, Tonya DelSontro, Avni Malhotra, Gustaf Hugelius, Guido Grosse, and Jennifer Watts for comments on an early draft of the figures and data analysis. M.A.K. received support from the Vanier Canada Graduate Scholarship and the W. Garfield Weston Foundation. D.O. received funding from the Campus Alberta Innovates Program, and the National Science and Engineering Research Council of Canada (NSERC) Discovery grant (RGPIN-2016-04688). D.B. was supported by the European Research Council (ERC; Horizon 2020 grant agreement 725546), the Swedish Research Council VR (2016-04829), and FORMAS (2018-01794). R.K.V. was supported by the US National Aeronautics and Space Administration (NNX17AK10G) and US Department of Energy (DE-SC0016440).

## References

Aben, R.C., Barros, N., Van Donk, E., Frenken, T., Hilt, S., Kazanjian, G., Lamers, L.P., Peeters, E.T., Roelofs, J.G., de Senerpont Domis, L.N. and Stephan, S.: Cross continental increase in methane ebullition under climate change, Nat. Commun., 8, 1682, <https://doi.org/10.1038/s41467-017-01535-y>, 2017.



- Andersen, R., Poulin, M., Borcard, D., Laiho, R., Laine, J., Vasander, H., and Tuittila, E. T: Environmental control and spatial structures in peatland vegetation, *Journal of Vegetation Science*, 22(5), 878-890, <https://doi.org/10.1111/j.1654-1103.2011.01295.x>, 2011.
- 755
- Bäckstrand, K., Crill, P.M., Mastepanov, M., Christensen, T.R. and Bastviken, D.: Total hydrocarbon flux dynamics at a subarctic mire in northern Sweden, *J. Geophys. Res.: Biogeosci.*, 113(G3), <https://doi.org/10.1029/2008JG000703>, 2008.
- Bartlett, K.B., Crill, P.M., Sass, R.L., Harriss, R.C. and Dise, N.B.: Methane emissions from tundra environments in the Yukon-Kuskokwim Delta, Alaska, *J. Geophys. Res.: Atmos.*, 97(D15), 16645-16660, <https://doi.org/10.1029/91JD00610>, 1992.
- 760
- Basiliko, N., Knowles, R., and Moore, T. R.: Roles of moss species and habitat in methane consumption potential in a northern peatland, *Wetlands*, 24(1), 178, [https://doi.org/10.1672/0277-5212\(2004\)024\[0178:ROMSAH\]2.0.CO;2](https://doi.org/10.1672/0277-5212(2004)024[0178:ROMSAH]2.0.CO;2), 2004.
- 765
- Bastviken, D., Ejlertsson, J., and Tranvik, L.: Measurement of methane oxidation in lakes: a comparison of methods, *Environ. Sci. & Technol.*, 36(15), 3354-3361, <https://doi.org/10.1021/es010311p>, 2002.
- Bastviken, D., Cole, J., Pace, M., and Tranvik, L.: Methane fluxes from lakes: Dependence of lake characteristics, two regional assessments, and a global estimate, *Global biogeochem. cycles*, 18(4), <https://doi.org/10.1029/2004GB002238>, 2004.
- 770
- Bastviken, D., Tranvik, L. J., Downing, J. A., Crill, P. M., and Enrich-Prast, A.: Freshwater methane fluxes offset the continental carbon sink, *Science*, 331(6013), 50-50, 2011.
- 775
- Beaulne, J., Garneau, M., Magnan, G., and Boucher, É.: Peat deposits store more carbon than trees in forested peatlands of the boreal biome, *Sci. Rep.*, 11, 2657, <https://doi.org/10.1038/s41598-021-82004-x>, 2021.
- Bellisario, L. M., Bubier, J. L., Moore, T. R., and Chanton, J. P: Controls on CH<sub>4</sub> fluxes from a northern peatland. *Global Biogeochem. Cycles*, 13(1), 81-91, <https://doi.org/10.1029/1998GB900021>, 1999.
- 780
- Belyea, L. R., and Baird, A. J.: Beyond “the limits to peat bog growth”: Cross-scale feedback in peatland development. *Ecological Monographs*, 76(3), 299-322, [https://doi.org/10.1890/0012-9615\(2006\)076\[0299:BTLTPB\]2.0.CO;2](https://doi.org/10.1890/0012-9615(2006)076[0299:BTLTPB]2.0.CO;2), 2006.



785

Bridgman, S. D., Cadillo-Quiroz, H., Keller, J. K., and Zhuang, Q.: Methane fluxes from wetlands: biogeochemical, microbial, and modeling perspectives from local to global scales, *Global Change Biology*, 19(5), 1325-1346, <https://doi.org/10.1111/gcb.12131>, 2013.

790

Brown, J., O. Ferrians, J. A. Heginbottom, and E. Melnikov. 2002. *Circum-Arctic Map of Permafrost and Ground-Ice Conditions, Version 2*. Boulder, Colorado USA. NSIDC: National Snow and Ice Data Center.  
doi: <https://doi.org/10.7265/skbg-kf16>. [11/20/2020]

795

Bruhwiller, L., Dlugokencky, E., Masarie, K., Ishizawa, M., Andrews, A., Miller, J., Sweeney, C., Tans, P., and Worthy, D.: CarbonTracker-CH<sub>4</sub>: an assimilation system for estimating emissions of atmospheric methane, *Atmos. Chem. Phys.*, 14, 8269–8293, <https://doi.org/10.5194/acp-14-8269-2014>, 2014.

800

Bubier, J. L., Moore, T. R., Bellisario, L., Comer, N. T., and Crill, P. M.: Ecological controls on methane fluxes from a northern peatland complex in the zone of discontinuous permafrost, Manitoba, Canada, *Global Biogeochem. Cycles*, 9(4), 455-470, <https://doi.org/10.1029/95GB02379>, 1995.

805

Canada Committee on Ecological (Biophysical) Land Classification, National Wetlands Working Group, Warner, B. G., and Rubec, C. D. A.: The Canadian wetland classification system, Wetlands Research Branch, University of Waterloo, Waterloo, Ont., 1997.

810

Christensen, T. R., Jonasson, S., Callaghan, T. V., and Havström, M.: Spatial variation in high-latitude methane flux along a transect across Siberian and European tundra environment, *J. Geophys. Res.: Atmos.*, 100(D10), 21035-21045, <https://doi.org/10.1029/95JD02145>, 1995

815

Christensen, T.R., Ekberg, A., Ström, L., Mastepanov, M., Panikov, N., Öquist, M., Svensson, B.H., Nykänen, H., Martikainen, P.J. and Oskarsson, H.: Factors controlling large scale variations in methane emissions from wetlands. *J. Geophys. Res. Lett.*, 30(7), <https://doi.org/10.1029/2002GL016848>, 2003.



- Cole, J. J., and Caraco, N. F.: Atmospheric exchange of carbon dioxide in a low-wind oligotrophic lake measured by the addition of SF<sub>6</sub>, *Limnol. Oceanogr.*, *43*(4), 647-656, <https://doi.org/10.4319/lo.1998.43.4.0647>, 1998.
- 820 Conrad, R., Claus, P., and Casper, P.: Characterization of stable isotope fractionation during methane production in the sediment of a eutrophic lake, Lake Dagow, Germany, *Limnol. Oceanogr.*, *54*(2), 457-471, <https://doi.org/10.4319/lo.2009.54.2.0457>, 2009.
- Czikowsky, M. J., S. MacIntyre, E. W. Tedford, J. Vidal, and S. D. Miller.: Effects of wind and buoyancy on carbon dioxide  
825 distribution and air-water flux of a stratified temperate lake, *J. Geophys. Res.: Biogeosci.* <https://doi.org/10.1029/2017JG004209>, 2018.
- DelSontro, T., Boutet, L., St-Pierre, A., del Giorgio, P. A., and Prairie, Y. T.: Methane ebullition and diffusion from northern  
830 ponds and lakes regulated by the interaction between temperature and system productivity. *Limnol. Oceanogr.*, *61*(S1), S62-S77, <https://doi.org/10.1002/lno.10335>, 2016.
- DelSontro, T., Beaulieu, J.J. and Downing, J.A.: Greenhouse gas emissions from lakes and impoundments: Upscaling in the face of global change, *Limnol. Oceanogr.*, *3*(3), pp.64-75, <https://doi.org/10.1002/lo.10073>, 2018.
- 835 Delwiche, K. B., Knox, S. H., Malhotra, A., Fluet-Chouinard, E., McNicol, G., Feron, S., Ouyang, Z., Papale, D., Trotta, C., Canfora, E., Cheah, Y.-W., Christianson, D., Alberto, M. C. R., Alekseychik, P., Aurela, M., Baldocchi, D., Bansal, S., Billesbach, D. P., Bohrer, G., Bracho, R., Buchmann, N., Campbell, D. I., Celis, G., Chen, J., Chen, W., Chu, H., Dalmagro, H. J., Dengel, S., Desai, A. R., Detto, M., Dolman, H., Eichelmann, E., Euskirchen, E., Famulari, D., Friborg, T., Fuchs, K., Goeckede, M., Gogo, S., Gondwe, M. J., Goodrich, J. P., Gottschalk, P., Graham, S. L., Heimann, M., Helbig, M., Helfter,  
840 C., Hemes, K. S., Hirano, T., Hollinger, D., Hörtnagl, L., Iwata, H., Jacotot, A., Jansen, J., Jurasinski, G., Kang, M., Kasak, K., King, J., Klatt, J., Koebisch, F., Krauss, K. W., Lai, D. Y. F., Mammarella, I., Manca, G., Marchesini, L. B., Matthes, J. H., Maximon, T., Merbold, L., Mitra, B., Morin, T. H., Nemitz, E., Nilsson, M. B., Niu, S., Oechel, W. C., Oikawa, P. Y., Ono, K., Peichl, M., Peltola, O., Reba, M. L., Richardson, A. D., Riley, W., Runkle, B. R. K., Ryu, Y., Sachs, T., Sakabe, A., Sanchez, C. R., Schuur, E. A., Schäfer, K. V. R., Sonnentag, O., Sparks, J. P., Stuart-Haëntjens, E., Sturtevant, C., Sullivan,  
845 R. C., Szutu, D. J., Thom, J. E., Torn, M. S., Tuittila, E.-S., Turner, J., Ueyama, M., Valach, A. C., Vargas, R., Varlagin, A., Vazquez-Lule, A., Verfaillie, J. G., Vesala, T., Vourlitis, G. L., Ward, E. J., Wille, C., Wohlfahrt, G., Wong, G. X., Zhang, Z., Zona, D., Windham-Myers, L., Poulter, B., and Jackson, R. B.: FLUXNET-CH<sub>4</sub>: A global, multi-ecosystem dataset and analysis of methane seasonality from freshwater wetlands, *Earth Syst. Sci. Data Discuss.* [preprint], <https://doi.org/10.5194/essd-2020-307>, in review, 2021.



- Dieleman, C.M., Rogers, B.M., Potter, S., Veraverbeke, S., Johnstone, J.F., Laflamme, J., Solvik, K., Walker, X.J., Mack, M.C. and Turetsky, M.R.: Wildfire combustion and carbon stocks in the southern Canadian boreal forest: Implications for a warming world, *Global Change Biology*, <https://doi.org/10.1111/gcb.15158>, 2020.
- 855 Downing, J. A., Cole, J. J., Duarte, C. M., Middelburg, J. J., Melack, J. M., Prairie, Y. T., Kortelainen, P., Striegl, R. G., McDowell, W. H., and Tranvik, L. J.: Global abundance and size distribution of streams and rivers, *Inland Waters*, 2, 229–236, <https://doi.org/10.5268/IW-2.4.502>, 2012.
- Elder, C.D., Xu, X., Walker, J., Schnell, J.L., Hinkel, K.M., Townsend-Small, A., Arp, C.D., Pohlman, J.W., Gaglioti, B.V.  
860 and Czimczik, C.I.: Greenhouse gas fluxes from diverse Arctic Alaskan lakes are dominated by young carbon. *Nat. Clim. Change* 8, 166–171, <https://doi.org/10.1038/s41558-017-0066-9>, 2018.
- Emmertson, C.A., St Louis, V.L., Lehnherr, I., Humphreys, E., Rydz, E. and Kosolofski, H.R.: The net exchange of methane with high Arctic landscapes during the summer growing season, *Biogeosciences*, 11(12), pp.3095-3106,  
865 <https://doi.org/10.5194/bg-11-3095-2014>, 2018.
- Fernández, E.J., Peeters, F. and Hofmann, H.: Importance of the autumn overturn and anoxic conditions in the hypolimnion for the annual methane emissions from a temperate lake, *Environ. Sci. Technol.*, 48(13), pp.7297-7304,  
<https://doi.org/10.1021/es4056164>, 2014.  
870
- von Fischer, J. C., Rhew, R. C., Ames, G. M., Fosdick, B. K., & von Fischer, P. E.: Vegetation height and other controls of spatial variability in methane fluxes from the Arctic coastal tundra at Barrow, Alaska, *J. Geophys. Res: Biogeosci.*, 115(G4), <https://doi.org/10.1029/2009JG001283>, 2010.
- 875 Frenzel, P., and Karofeld, E.: CH<sub>4</sub> flux from a hollow-ridge complex in a raised bog: The role of CH<sub>4</sub> production and oxidation, *Biogeochemistry* 51, 91–112, <https://doi.org/10.1023/A:1006351118347>, 2000.
- Garneau, M., Tremblay, L., and Magnan, G.: Holocene pool formation in oligotrophic fens from boreal Québec in northeastern Canada, *The Holocene*, 28, 396–407, <https://doi.org/10.1177/0959683617729439>, 2018.
- 880 Glaser, P. H., Siegel, D. I., Reeve, A. S., Janssens, J. A., and Janecky, D. R.: Tectonic drivers for vegetation patterning and landscape evolution in the Albany River region of the Hudson Bay Lowlands, *J. Ecol.*, 92, 1054–1070, <https://doi.org/10.1111/j.0022-0477.2004.00930.x>, 2004.



- 885 Gorham, E: Northern peatlands: role in the carbon cycle and probable responses to climatic warming, *Ecological applications*, 1(2), pp.182-195, 1991.
- Grossart, H.P., Frindte, K., Dziallas, C., Eckert, W. and Tang, K.W.: Microbial methane production in oxygenated water column of an oligotrophic lake, *Proc. Natl. Acad. Sci.*, 108(49), pp.19657-19661, <https://doi.org/10.1073/pnas.1110716108>,  
890 2011.
- Gunnarsson, U. and Löfroth, M.: The Swedish wetland survey: compiled excerpts from the national final report. Swedish Environmental Protection Agency, 2014.
- 895 Harris, L. I., Roulet, N. T., and Moore, T. R.: Mechanisms for the Development of Microform Patterns in Peatlands of the Hudson Bay Lowland, *Ecosystems*, 23, 741–767, <https://doi.org/10.1007/s10021-019-00436-z>, 2020.
- Heikkinen, J.E., Virtanen, T., Huttunen, J.T., Elsakov, V. and Martikainen, P.J.: Carbon balance in East European tundra. *Global Biogeochem. Cycles*, 18(1), 2004.  
900
- Heiskanen, J. J., I. Mammarella, S. Haapanala, J. Pumpanen, T. Vesala, S. MacIntyre, and A. Ojala.: Effects of cooling and internal wave motions on gas transfer coefficients in a boreal lake, *Tellus B* 66:22827, <http://dx.doi.org/10.3402/tellusb.v66.22827>, 2014.  
905
- Heiskanen, L., Tuovinen, J.-P., Räsänen, A., Virtanen, T., Juutinen, S., Lohila, A., Penttilä, T., Linkosalmi, M., Mikola, J., Laurila, T., and Aurela, M.: Carbon dioxide and methane exchange of a patterned subarctic fen during two contrasting growing seasons, *Biogeosciences*, 18, 873–896, <https://doi.org/10.5194/bg-18-873-2021>, 2021.
- 910 Holgerson, M., and Raymond, P.: Large contribution to inland water CO<sub>2</sub> and CH<sub>4</sub> fluxes from very small ponds, *Nat. Geosci.*, 9, 222–226, <https://doi.org/10.1038/ngeo2654>, 2016.
- van Huissteden, J., Maximov, T. C., and Dolman, A. J.: High methane flux from an arctic floodplain (Indigirka lowlands, eastern Siberia), *J. Geo. Res.: Biogeosciences*, 110(G2), <https://doi.org/10.1029/2005JG000010>, 2005.  
915
- Jansen, J., Thornton, B. F., Wik, M., MacIntyre, S., and Crill, P. M.: Temperature proxies as a solution to biased sampling of lake methane fluxes, *Geophys. Res. Letters*, 47(14), <https://doi.org/10.1029/2020GL088647>, 2020.



- Jorgenson, M. T., Racine, C. H., Walters, J. C., and Osterkamp, T. E.: Permafrost Degradation and Ecological Changes  
920 Associated with a Warming Climate in Central Alaska, *Climatic Change*, 48, 551–579,  
<https://doi.org/10.1023/A:1005667424292>, 2001.
- Juutinen, S., Alm, J., Larmola, T., Huttunen, J. T., Morero, M., Martikainen, P. J., and Silvola, J.: Major implication of the  
littoral zone for methane release from boreal lakes, 17, <https://doi.org/10.1029/2003GB002105>, 2003.
- 925
- Karlsson, J., Giesler, R., Persson, J. and Lundin, E.: High emission of carbon dioxide and methane during ice thaw in high  
latitude lakes. *Geophys. Res. Letters*, 40(6), pp.1123-1127, <https://doi.org/10.1002/grl.50152>, 2013.
- Kelly, C. A., and Chynoweth, D. P.: The contributions of temperature and of the input of organic matter in controlling rates  
930 of sediment methanogenesis 1, *Limnol. Oceanogr.*, 26(5), 891-897, <https://doi.org/10.4319/lo.1981.26.5.0891>, 1981.
- Klaus, M., Bergström, A.K., Jonsson, A., Deiningner, A., Geibrink, E. and Karlsson, J.: Weak response of greenhouse gas  
emissions to whole lake N enrichment, *Limnol. Oceanogr.*, 63(S1), pp.S340-S353, <https://doi.org/10.1002/lno.10743>, 2018.
- 935
- Knox, S.H., Jackson, R.B., Poulter, B., McNicol, G., Fluet-Chouinard, E., Zhang, Z., Hugelius, G., Bousquet, P., Canadell,  
J.G., Saunois, M. and Papale, D.: FLUXNET-CH4 synthesis activity: Objectives, observations, and future directions, *Bull.*  
*Amer. Meteor. Soc.* (2019) 100 (12): 2607–2632, <https://doi.org/10.1175/BAMS-D-18-0268.1>, 2019.
- Kuhn, M., Lundin, E.J., Giesler, R., Johansson, M. and Karlsson, J.: Emissions from thaw ponds largely offset the carbon  
940 sink of northern permafrost wetlands, *Scientific Reports*, 8(1), pp.1-7, <https://doi.org/10.1038/s41598-018-27770-x>, 2018.
- Larmola, T., Tuittila, E.S., Tirola, M., Nykänen, H., Martikainen, P.J., Yrjälä, K., Tuomivirta, T. and Fritze, H.: The role of  
Sphagnum mosses in the methane cycling of a boreal mire, *Ecology*, 91(8), pp.2356-2365, <https://doi.org/10.1890/09-1343.1>, 2010.
- 945
- Li, M., Peng, C., Zhu, Q., Zhou, X., Yang, G., Song, X. and Zhang, K.: The significant contribution of lake depth in  
regulating global lake diffusive methane emissions, *Water Research*, 172, p.115465,  
<https://doi.org/10.1016/j.watres.2020.115465>, 2020.



- 950 Machacova, K., Bäck, J., Vanhatalo, A., Halmeenmäki, E., Kolari, P., Mammarella, I., Pumpanen, J., Acosta, M., Urban, O.,  
and Pihlatie, M.: Pinus sylvestris as a missing source of nitrous oxide and methane in boreal forest, *Sci. Rep.*, 6, 23410,  
<https://doi.org/10.1038/srep23410>, 2016.
- MacIntyre, S., Crowe, A.T., Cortés, A. and Arneborg, L.: Turbulence in a small arctic pond, *Limnol. Oceanogr.*, 63(6),  
955 pp.2337-2358, <https://doi.org/10.1002/lno.10941>, 2018.
- MacIntyre, S., Bastviken, D., Arneborg, L., Crow, A. T., Karlsson, J., Andersson, A., Galfalk, M., Rutgersson, A.,  
Podgrajsek, E., and Melack, J. M.: Turbulence in a small boreal lake: Consequences for air-water gas exchange, *Limnol.  
Oceanogr.*, 9999, 1-28., <https://doi.org/10.1002/lno.11645>, 2020.
- 960 Markfort, C. D., A. L. S. Perez, J. W. Thill, D. A. Jaster, F. Porte-Agel, and H. G. Stefan.: Wind sheltering of a lake by a tree  
canopy or bluff topography, *Water Resources. Res.*, 46: W03530, <https://doi.org/10.1029/2009WR007759>, 2010.
- Masing, V., Botch, M., and Läänelaid, A.: Mires of the former Soviet Union, *Wetlands Ecol. Manage.*, 18, 397–433,  
965 <https://doi.org/10.1007/s11273-008-9130-6>, 2010.
- Matson, A., Pennock, D., and Bedard-Haughn, A.: Methane and nitrous oxide emissions from mature forest stands in the  
boreal forest, Saskatchewan, Canada, *For. Ecol. Manage.*, 258, 1073–1083, <https://doi.org/10.1016/j.foreco.2009.05.034>,  
2009.
- 970 Muster, S., Riley, W. J., Roth, K., Langer, M., Cresto Aleina, F., Koven, C. D., Lange, S., Bartsch, A., Grosse, G., Wilson,  
C. J., Jones, B. M., and Boike, J.: Size Distributions of Arctic Waterbodies Reveal Consistent Relations in Their Statistical  
Moments in Space and Time, *Front. Earth Sci.*, 7, <https://doi.org/10.3389/feart.2019.00005>, 2019.
- 975 Kip, N., Van Winden, J.F., Pan, Y., Bodrossy, L., Reichart, G.J., Smolders, A.J., Jetten, M.S., Damsté, J.S.S. and Den Camp,  
H.J.O.: Global prevalence of methane oxidation by symbiotic bacteria in peat-moss ecosystems, *Nat. Geosci.* 3, 617–621,  
<https://doi.org/10.1038/ngeo939>, 2010.
- Le Mer, J. and Roger, P.: Production, oxidation, flux and consumption of methane by soils: a review, *European journal of*  
980 *soil biology*, 37(1), pp.25-50, [https://doi.org/10.1016/S1164-5563\(01\)01067-6](https://doi.org/10.1016/S1164-5563(01)01067-6), 2001.
- Lehner, B., and Döll, P.: Development and validation of a global database of lakes, reservoirs and wetlands, *J.  
Hydrol.*, 296(1-4), 1-22, <https://doi.org/10.1016/j.jhydrol.2004.03.028>, 2004.



- 985 Li, M., Peng, C., Zhu, Q., Zhou, X., Yang, G., Song, X., & Zhang, K.: The significant contribution of lake depth in regulating global lake diffusive methane emissions, *Water research*, 172, 115465, <https://doi.org/10.1016/j.watres.2020.115465>, 2020.
- Liljedahl, A. K., Boike, J., Daanen, R. P., Fedorov, A. N., Frost, G. V., Grosse, G., Hinzman, L. D., Iijma, Y., Jorgenson, J.,  
990 C., Matveyeva, N., Necsoiu, M., Reynolds, M. K., Romanovsky, V. E., Schulla, J., Tape, K. D., Walker, D. A., Wilson, C. J., Yabuki, H., and Zona, D.: Pan-Arctic ice-wedge degradation in warming permafrost and its influence on tundra hydrology, *Nat. Geosci.*, 9, 312–318, <https://doi.org/10.1038/ngeo2674>, 2016.
- Machacova, K., Bäck, J., Vanhatalo, A., Halmeenmäki, E., Kolari, P., Mammarella, I., Pumpanen, J., Acosta, M., Urban, O.,  
995 and Pihlatie, M.: *Pinus sylvestris* as a missing source of nitrous oxide and methane in boreal forest, *Sci. Rep.*, 6, 23410, <https://doi.org/10.1038/srep23410>, 2016.
- Malhotra, A. and Roulet, N. T.: Environmental correlates of peatland carbon fluxes in a thawing landscape: do transitional thaw stages matter?, *Biogeosci.*, 12, 3119–3130, <https://doi.org/10.5194/bg-12-3119-2015>, 2015.
- Mammarella, I., Nordbo, A., Rannik, Ü., Haapanala, S., Levula, J., Laakso, H., Ojala, A., Peltola, O., Heiskanen, J.,  
1000 Pumpanen, J. and Vesala, T.: Carbon dioxide and energy fluxes over a small boreal lake in Southern Finland, *J. Geophys. Res.: Biogeosci.*, 120(7), pp.1296-1314, <https://doi.org/10.1002/2014JG002873>, 2015.
- Marinho, C. C., Palma-Silva, C., Albertoni, E. F., Giacomini, I. B., Barros, M. P. F., Furlanetto, L. M., and de Assis Esteves, F.: Emergent macrophytes alter the sediment composition in a small, shallow subtropical lake: Implications for methane flux, *Am. J. Plant Sci.*, 6(02), 315, <https://doi.org/10.4236/ajps.2015.62036>, 2015.  
1005
- Matthews, E., and Fung, I.: Methane flux from natural wetlands: Global distribution, area, and environmental characteristics of sources. *Global Biogeochem. Cycles*, 1(1), 61-86, <https://doi.org/10.1029/GB001i001p00061>, 1987.
- Matthews, E., Johnson, M. S., Genovese, V., Du, J., and Bastviken, D.: Methane flux from high latitude lakes: methane-centric lake classification and satellite-driven annual cycle of fluxes, *Scientific Reports*, 10(1), 1-9, 2020.  
1010
- Matveev, A., Laurion, I., Deshpande, B. N., Bhiry, N., & Vincent, W. F.: High methane fluxes from thermokarst lakes in subarctic peatlands, *Limnol. Oceanogr.*, 61(S1), S150-S164, <https://doi.org/10.1002/lno.10311>, 2016.



1015 Mazerolle, M. J., & Mazerolle, M. M. J.: Package “AICcmodavg” AICcmodavg; model selection and multimodel inference based on(Q) AIC ©. CRAN R Project, 2015.

McCalley, C.K., Woodcroft, B.J., Hodgkins, S.B., Wehr, R.A., Kim, E.H., Mondav, R., Crill, P.M., Chanton, J.P., Rich, V.I., Tyson, G.W. and Saleska, S.R.: Methane dynamics regulated by microbial community response to permafrost  
1020 thaw. *Nature*, 514, 478-481, <https://doi.org/10.1038/nature13798>, 2014.

McGuire, A.D., Christensen, T.R., Hayes, D.J., Heroult, A., Euskirchen, E., Yi, Y., Kimball, J.S., Koven, C., Lafleur, P., Miller, P.A. and Oechel, W.: An assessment of the carbon balance of Arctic tundra: comparisons among observations, process models, and atmospheric inversions. *Biogeosciences Discussions*, 9, p.4543, [http://dx.doi.org/10.5194/bg-9-3185-](http://dx.doi.org/10.5194/bg-9-3185-2012)  
1025 2012, 2012.

Melton, J., Wania, R., Hodson, E.L., Poulter, B., Ringeval, B., Spahni, R., Bohn, T., Avis, C., Beerling, D., Chen, G. and Eliseev, A.: Present state of global wetland extent and wetland methane modeling : conclusions from a model inter-comparison project (WETCHIMP), *Biogeosciences*, 10, 753–788, <https://doi.org/10.5194/bg-10-753-2013>, 2013.

1030 Messenger, M. L., Lehner, B., Grill, G., Nedeva, I., and Schmitt, O.: Estimating the volume and age of water stored in global lakes using a geo-statistical approach. *Nat. Commun.*, 7, 13603, <https://doi.org/10.1038/ncomms13603>, 2016.

van der Molen, M.K., Van Huissteden, J., Parmentier, F.J.W., Petrescu, A.M.R., Dolman, A.J., Maximov, T.C., Kononov, A.V., Karsanaev, S.V. and Suzdalov, D.A.: The growing season greenhouse gas balance of a continental tundra site in the Indigirka lowlands, NE Siberia, *Biogeosciences*, 2007.

Moore, T. R., Heyes, A., and Roulet, N. T.: Methane fluxes from wetlands, southern Hudson Bay lowland, *J. Geophys. Res.: Atmos.*, 99 (D1), 1455-1467, <https://doi.org/10.1029/93JD02457>, 1994.

1040 Moosavi, S.C. and Crill, P.M.: Controls on CH<sub>4</sub> and CO<sub>2</sub> emissions along two moisture gradients in the Canadian boreal zone, *J. Geophys. Res.: Atmos.*, 102(D24), pp.29261-29277, <https://doi.org/10.1029/96JD03873>, 1997.

National Wetlands Working Group (NWWG): The Canadian Wetland Classification System, 2nd Edition. Warner, B.G. and  
1045 C.D.A. Rubec (eds.), Wetlands Research Centre, University of Waterloo, Waterloo, ON, Canada. 68 p., 1997.



- Nielsen, C. S., Hasselquist, N. J., Nilsson, M. B., Öquist, M., Järveoja, J., and Peichl, M.: A Novel Approach for High-Frequency in-situ Quantification of Methane Oxidation in Peatlands. *Soil Syst.*, 3(1), 4, <https://doi.org/10.3390/soilsystems3010004>, 2019.
- 1050
- Nykänen, H., Heikkinen, J. E., Pirinen, L., Tiilikainen, K., and Martikainen, P. J.: Annual CO<sub>2</sub> exchange and CH<sub>4</sub> fluxes on a subarctic palsamire during climatically different years, *Global Biogeochem. Cycles*, 17(1), 2003.
- Oh, Y., Zhuang, Q., Liu, L., Welp, L.R., Lau, M.C., Onstott, T.C., Medvigy, D., Bruhwiler, L., Dlugokencky, E.J., Hugelius, G. and D'Imperio, L.: Reduced net methane emissions due to microbial methane oxidation in a warmer Arctic, *Nat. Clim. Change*. 10, 317–321, <https://doi.org/10.1038/s41558-020-0734-z>, 2020.
- 1055
- Olefeldt, D., Turetsky, M. R., Crill, P. M., and McGuire, A. D.: Environmental and physical controls on northern terrestrial methane fluxes across permafrost zones. *Global Change Biology*, 19(2), 589-603, <https://doi.org/10.1111/gcb.12071>, 2013.
- 1060
- Olefeldt, D., Euskirchen, E. S., Harden, J., Kane, E., McGuire, A. D., Waldrop, M. P., and Turetsky, M. R.: A decade of boreal rich fen greenhouse gas fluxes in response to natural and experimental water table variability. *Global Change biology*, 23(6), 2428-2440, <https://doi.org/10.1111/gcb.13612>, 2017.
- 1065
- Olefeldt, D., Hovemyr, M., Kuhn, M.A., Bastviken, D., Bohn, T., Connolly, J., Crill, P., Euskirchen, E., Finklestein, S., Genet, H., Grosse, G., Harris, L., Heffernan, L., Helbig, M., Hugelius, G., Hutchins, R., Juutinen, S., Lara, M., Malhotra, A., Manies, K., McGuire, A.D., Natali, S., O'Donnell, S., Parmentier, F.J., Räsänen, A., Schaedel, C., Sonnentag, O., Strack, M., Tank, S., Treat, C., Varner, R.K., Virtanen, T., Warren, R., Watts, J.D.: The fractional land cover estimates from the Boreal-Arctic Wetland and Lake Dataset (BAWLD), 2021. Arctic Data Center [data set], <https://doi.org/10.18739/A2C824F9X>, 2021.
- 1070
- Olson, D.M., Dinerstein, E., Wikramanayake, E.D., Burgess, N.D., Powell, G.V., Underwood, E.C., D'Amico, J.A., Itoua, I., Strand, H.E., Morrison, J.C. and Loucks, C.J.: Terrestrial Ecoregions of the World: A New Map of Life on Earth A new global map of terrestrial ecoregions provides an innovative tool for conserving biodiversity. *BioScience*, 51(11), 933-938, [https://doi.org/10.1641/0006-3568\(2001\)051\[0933:TEOTWA\]2.0.CO;2](https://doi.org/10.1641/0006-3568(2001)051[0933:TEOTWA]2.0.CO;2), 2001.
- 1075
- Öquist, M. G., and Svensson, B. H.: Vascular plants as regulators of methane fluxes from a subarctic mire ecosystem, *J. Geophys. Res.: Atmos.*, 107(D21), ACL-10, <https://doi.org/10.1029/2001JD001030>, 2002.



1080 Peltola, O., Vesala, T., Gao, Y., Rätty, O., Alekseychik, P., Aurela, M., Chojnicki, B., Desai, A.R., Dolman, A.J., Euskirchen, E.S. and Friborg, T.: Monthly gridded data product of northern wetland methane fluxes based on upscaling eddy covariance observations, *Earth system Science Data*, *11*(3), pp.1263-1289, <https://doi.org/10.5194/essd-11-1263-2019>, 2019.

Peeters, F., Fernandez, J.E. and Hofmann, H.: Sediment fluxes rather than oxic methanogenesis explain diffusive CH<sub>4</sub> emissions from lakes and reservoirs. *Scientific Reports*, *9*(1), pp.1-10, <https://doi.org/10.1038/s41598-018-36530-w>, 2019.

Perryman, C.R., McCalley, C.K., Malhotra, A., Fahnestock, M.F., Kashi, N.N., Bryce, J.G., Giesler, R. and Varner, R.K.: Thaw Transitions and Redox Conditions Drive Methane Oxidation in a Permafrost Peatland, *Journal of Geophysical Research: Biogeosciences*, *125*(3), p.e2019JG005526, <https://doi.org/10.1029/2019JG005526>, 2020.

1090

Pinheiro, J., Bates, D., DebRoy, S., Sarkar, D., Heisterkamp, S., Van, Willigen, B., & Maintainer, R: Package “nlme”. Linear and Nonlinear Mixed Effects Models, version 3-1. CRAN R Project, 2017.

Popp, T.J., Chanton, J.P., Whiting, G.J. and Grant, N.: Evaluation of methane oxidation in the rhizosphere of a *Carex* dominated fen in northcentral Alberta, Canada, *Biogeochemistry*, *51*(3), pp.259-281, <https://doi.org/10.1023/A:1006452609284>, 2000

Ramsar Convention Secretariat (RCS) (previously The Ramsar Convention Manual): An Introduction to the Convention on Wetlands, Gland, Switzerland, 2016.

1100

Rasilo, T., Prairie, Y. T., and del Giorgio, P. A.: Large-scale patterns in summer diffusive CH<sub>4</sub> fluxes across boreal lakes, and contribution to diffusive C fluxes. *Global Change Biology*, *21*(3), 1124-1139, <https://doi.org/10.1111/gcb.12741>, 2015.

1105 Sannel, A. B. K. and Kuhry, P.: Warming-induced destabilization of peat plateau/thermokarst lake complexes, *J. Geophys. Res.: Biogeosci.*, *116*, <https://doi.org/10.1029/2010JG001635>, 2011.

Saunio, M., Stavert, A.R., Poulter, B., Bousquet, P., Canadell, J.G., Jackson, R.B., Raymond, P.A., Dlugokencky, E.J., Houweling, S., Patra, P.K. and Ciais, P.: The global methane budget 2000–2017, *Earth Sys. Sci. Data*, *12*(3), pp.1561-1623, <https://doi.org/10.5194/essd-12-1561-2020>, 2020.

Schirrmeister, L., Froese, D., Tumskey, V., Grosse, G. and Wetterich, S.: Yedoma: Late Pleistocene ice-rich syngenetic permafrost of Beringia, *Encyclopedia of Quaternary Science*. 2nd edition (pp. 542-552), doi: 10.1016/B978-0-444-53643-3.00106-0, 2013.



1115

Schnurrenberger, D., Russell, J., and Kelts, K.: Classification of lacustrine sediments based on sedimentary components, *J. Paleolimnology*, 29(2), 141-154, <https://doi.org/10.1023/A:1023270324800>, 2003.

1120

Segarra, K.E.A., Schubotz, F., Samarkin, V., Yoshinaga, M.Y., Hinrichs, K.U. and Joye, S.B.: High rates of anaerobic methane oxidation in freshwater wetlands reduce potential atmospheric methane emissions, *Nat. Comm.*, 6(1), pp.1-8, <https://doi.org/10.1038/ncomms8477>, 2015.

1125

Sepulveda-Jauregui, A., Walter Anthony, K.M., Martinez-Cruz, K., Greene, S. and Thalasso, F.: Methane and carbon dioxide emissions from 40 lakes along a north–south latitudinal transect in Alaska, *Biogeosci. Discuss*, 11(9), pp.13251-13307, doi:10.5194/bgd-11-13251-2014, 2014.

Smith, K.B., C.E. Smith, S.F. Forest, and A.J. Richard.: *A Field Guide to the Wetlands of the Boreal Plains Ecozone of Canada*. Ducks Unlimited Canada, Western Boreal Office: Edmonton, Alberta. 98 pp, 2007.

1130

Spahni, R., Wania, R., Neef, L., van Weele, M., Pison, I., Bousquet, P., Frankenberg, C., Foster, P. N., Joos, F., Prentice, I. C., and van Velthoven, P.: Constraining global methane emissions and uptake by ecosystems, *Biogeosciences*, 8, 1643–1665, <https://doi.org/10.5194/bg-8-1643-2011>, 2011.

1135

Stanley, E. H., Casson, N. J., Christel, S. T., Crawford, J. T., Loken, L. C., and Oliver, S. K.: The ecology of methane in streams and rivers: patterns, controls, and global significance, *Ecological Monographs*, 86(2), 146-171, <https://doi.org/10.1890/15-1027>, 2016.

1140

Strauss, J., Schirrmeister, L., Grosse, G., Fortier, D., Hugelius, G., Knoblauch, C., Romanovsky, V., Schädel, C., von Deimling, T.S., Schuur, E.A. and Shmelev, D.: Deep Yedoma permafrost: A synthesis of depositional characteristics and carbon vulnerability. *Earth-Science Reviews*, 172, pp.75-86, <https://doi.org/10.1016/j.earscirev.2017.07.007>, 2017.

Ström, L., and Christensen, T. R.: Below ground carbon turnover and greenhouse gas exchanges in a sub-arctic wetland. *Soil Biology and Biochemistry*, 39(7), 1689-1698, <https://doi.org/10.1016/j.soilbio.2007.01.019>, 2007.

1145

Ström, L., Mastepanov, M., and Christensen, T. R.: Species-specific effects of vascular plants on carbon turnover and methane fluxes from wetlands. *Biogeochemistry*, 75(1), 65-82, <https://doi.org/10.1007/s10533-004-6124-1>, 2005.



- Ström, L., Tagesson, T., Mastepanov, M., and Christensen, T. R.: Presence of *Eriophorum scheuchzeri* enhances substrate availability and methane flux in an Arctic wetland. *Soil Biol. Biochem.*, *45*, 61-70,  
1150 <https://doi.org/10.1016/j.soilbio.2011.09.005>, 2012.
- Tan, Z.L., Zhuang, Q.L., Henze, D.K., Frankenberg, C., Dlugokencky, E., Sweeney, C., Turner, A.J., Sasakawa, M. and Machida, T.: Inverse modeling of pan-Arctic methane fluxes at high spatial resolution: what can we learn from assimilating satellite retrievals and using different process-based wetland and lake biogeochemical models, *Atmos. Chem. Phys.*,  
1155 <http://dx.doi.org/10.5194/acp-16-12649-2016>, 2016.
- Thompson, R.L., Nisbet, E.G., Pisso, I., Stohl, A., Blake, D., Dlugokencky, E.J., Helmig, D. and White, J.W.C.: Variability in atmospheric methane from fossil fuel and microbial sources over the last three decades. *J. Geophys. Res.: Letters*, *45*(20), pp.11-499, <https://doi.org/10.1029/2018GL078127>, 2018.  
1160
- Thornton, B. F., Wik, M., and Crill, P. M.: Climate-forced changes in available energy and methane bubbling from subarctic lakes, *Geophys. Res.: Letters*, *42*(6), 1936-1942, <https://doi.org/10.1002/2015GL063189> 2015.
- Thornton, B.G., Wik, M., and Crill, P.M.: Double-counting challenges the accuracy of high latitude methane inventories, *Geophys. Res. Lett.*, *43*(12), <https://doi.org/10.1002/2016GL071772>, 2016.  
1165
- Terentieva, I.E., Glagolev, M.V., Lapshina, E.D., Sabrekov, A.F. and Maksyutov, S.: Mapping of West Siberian taiga wetland complexes using Landsat imagery: implications for methane emissions. *Biogeosciences*, *13*(16), p.4615,  
1170 [doi:10.5194/bg-13-4615-2016](https://doi.org/10.5194/bg-13-4615-2016), 2016.
- Treat, C. C., Bloom, A. A., and Marushchak, M. E.: Nongrowing season methane fluxes—a significant component of annual fluxes across northern ecosystems. *Global Change Biology*, *24*(8), 3331-3343, <https://doi.org/10.1111/gcb.14137>, 2018.
- Turetsky, M. R., Wieder, R. K., and Vitt, D. H.: Boreal peatland C fluxes under varying permafrost regimes, *Soil Biology and Biochemistry*, *34*, 907–912, [https://doi.org/10.1016/S0038-0717\(02\)00022-6](https://doi.org/10.1016/S0038-0717(02)00022-6), 2002.  
1175
- Turetsky, M.R., Kotowska, A., Bubier, J., Dise, N.B., Crill, P., Hornibrook, E.R., Minkinen, K., Moore, T.R., Myers-Smith, I.H., Nykänen, H. and Olefeldt, D.: A synthesis of methane fluxes from 71 northern, temperate, and subtropical wetlands, *Global Change Biology*, *20*(7), pp.2183-2197, <https://doi.org/10.1111/gcb.12580>, 2014.  
1180
- Virtanen, R., Oksanen, L., Oksanen, T., Cohen, J., Forbes, B. C., Johansen, B., Käyhkö, J., Olofsson, J., Pulliainen, J., and Tømmervik, H.: Where do the treeless tundra areas of northern highlands fit in the global biome system: toward an



ecologically natural subdivision of the tundra biome, *Ecology and Evolution*, 6, 143–158, <https://doi.org/10.1002/ece3.1837>, 2016.

1185

Virtanen, T. and Ek, M.: The fragmented nature of tundra landscape, *Int. J. of Applied Earth Observation and Geoinformation*, 27, 4–12, <https://doi.org/10.1016/j.jag.2013.05.010>, 2014.

1190 Wagner, D., Kobabe, S., Pfeiffer, E.M. and Hubberten, H.W.: Microbial controls on methane fluxes from a polygonal tundra of the Lena Delta, Siberia. *Permafrost. Periglac. Process.*, 14(2), 173-185, <https://doi.org/10.1002/ppp.443>, 2003.

Walter, K. M., Zimov, S. A., Chanton, J. P., Verbyla, D., and Chapin, F. S.: Methane bubbling from Siberian thaw lakes as a positive feedback to climate warming. *Nature*, 443(7107), 71-75, <https://doi.org/10.1038/nature05040>, 2006.

1195 Walter Anthony, K.M., Vas, D.A., Brosius, L., Chapin III, F.S., Zimov, S.A. and Zhuang, Q.: Estimating methane emissions from northern lakes using ice-bubble surveys. *Limnol. Oceanogr.: Methods*, 8(11), pp.592-609, <https://doi.org/10.4319/lom.2010.8.0592>, 2010.

1200 Walter Anthony, K., Daanen, R., Anthony, P., von Deimling, T. S., Ping, C. L., Chanton, J. P., and Grosse, G.: Methane fluxes proportional to permafrost carbon thawed in Arctic lakes since the 1950s, *Nat. Geosci.*, 9, 679–682, <https://doi.org/10.1038/ngeo2795>, 2016.

1205 Watson, A., Stephen, K.D., Nedwell, D.B. and Arah, J.R.: Oxidation of methane in peat: kinetics of CH<sub>4</sub> and O<sub>2</sub> removal and the role of plant roots, *Soil Biol. Biochem.*, 29(8), pp.1257-1267, [https://doi.org/10.1016/S0038-0717\(97\)00016-3](https://doi.org/10.1016/S0038-0717(97)00016-3), 1997.

Watts, J. D., Kimball, J. S., Bartsch, A., and McDonald, K. C.: Surface water inundation in the boreal-Arctic: potential impacts on regional methane fluxes, *Environ. Res. Letters*, 9(7), 075001, 2014.

1210 Wessel, P., and W. H. F. Smith: A global, self-consistent, hierarchical, high-resolution shoreline database, *J. Geophys. Res.*, 101(B4), 8741–8743, doi:10.1029/96JB00104, 1996.

Whalen, S. C.: Biogeochemistry of methane exchange between natural wetlands and the atmosphere. *Environmental Engineering Science*, 22(1), 73-94, <https://doi.org/10.1089/ees.2005.22.73>, 2005.



- 1215 Wik, M., Crill, P. M., Varner, R. K., and Bastviken, D.: Multiyear measurements of ebullitive methane flux from three subarctic lakes. *J. Geophys. Res.: Biogeosci.*, *118*(3), 1307-1321, <https://doi.org/10.1002/jgrg.20103>, 2013.
- Wik, M., Thornton, B. F., Bastviken, D., MacIntyre, S., Varner, R. K., and Crill, P. M.: Energy input is primary controller of methane bubbling in subarctic lakes. *J. Geophys. Res. Letters*, *41*(2), 555-560, <https://doi.org/10.1002/2013GL058510>, 2014.
- 1220 Wik, M., Thornton, B. F., Bastviken, D., Uhlbäck, J., and Crill, P. M.: Biased sampling of methane release from northern lakes: A problem for extrapolation, *J. Geophys. Res.: Letters*, *43*(3), 1256-1262, <https://doi.org/10.1002/2015GL066501>, 2016a.
- 1225 Wik, M., Varner, R. K., Anthony, K. W., MacIntyre, S., & Bastviken, D.: Climate-sensitive northern lakes and ponds are critical components of methane release, *Nat. Geosci.*, *9*, 99–105, <https://doi.org/10.1038/ngeo2578>, 2016b.
- Wik, M., Johnson, J.E., Crill, P.M., DeStasio, J.P., Erickson, L., Halloran, M.J., Fahnestock, M.F., Crawford, M.K., Phillips, S.C. and Varner, R.K.: Sediment characteristics and methane ebullition in three subarctic lakes, *J. Geophys. Res.:*
- 1230 *Biogeosci.*, *123*(8), pp.2399-2411, <https://doi.org/10.1029/2017JG004298>, 2018.
- Woodcroft, B.J., Singleton, C.M., Boyd, J.A., Evans, P.N., Emerson, J.B., Zayed, A.A., Hoelzle, R.D., Lamberton, T.O., McCalley, C.K., Hodgkins, S.B. and Wilson, R.M.: 2018. Genome-centric view of carbon processing in thawing permafrost, *Nature*, *560*(7716), 49-54, <https://doi.org/10.1038/s41586-018-0338-1>, 2018.
- 1235 Yvon-Durocher, G., Allen, A.P., Bastviken, D., Conrad, R., Gudas, C., St-Pierre, A., Thanh-Duc, N. and Del Giorgio, P.A.: Methane fluxes show consistent temperature dependence across microbial to ecosystem scales. *Nature*, *507*(7493), pp.488-491, <https://doi.org/10.1038/nature13164>, 2014.
- 1240 Zhu, X., Zhuang, Q., Qin, Z., Glagolev, M., and Song, L.: Estimating wetland methane fluxes from the northern high latitudes from 1990 to 2009 using artificial neural networks, *Global Biogeochem/ Cycles*, *27*(2), 592-604, <https://doi.org/10.1002/gbc.20052>, 2013.
- Zona, D., Gioli, B., Commane, R., Lindaas, J., Wofsy, S.C., Miller, C.E., Dinardo, S.J., Dengel, S., Sweeney, C., Karion, A.
- 1245 and Chang, R.Y.W.: Cold season fluxes dominate the Arctic tundra methane budget, *Proc. Natl. Acad. Sci.*, *113*(1), pp.40-45, <https://doi.org/10.1073/pnas.1516017113>, 2016.